
Efficient Preference Poisoning Attack on Offline RLHF

Chenye Yang¹ Weiyu Xu² Lifeng Lai¹

Abstract

Offline Reinforcement Learning from Human Feedback (RLHF) pipelines such as Direct Preference Optimization (DPO) train on a pre-collected preference dataset, which makes them vulnerable to preference poisoning attack. We study label flip attacks against log-linear DPO. We first illustrate that flipping one preference label induces a parameter-independent shift in the DPO gradient. Using this key property, we can then convert the targeted poisoning problem into a structured binary sparse approximation problem. To solve this problem, we develop two attack methods: Binary-Aware Lattice Attack (BAL-A) and Binary Matching Pursuit Attack (BMP-A). BAL-A embeds the binary flip selection problem into a binary-aware lattice and applies Lenstra-Lenstra-Lovász reduction and Babai’s nearest plane algorithm; we provide sufficient conditions that enforce binary coefficients and recover the minimum-flip objective. BMP-A adapts binary matching pursuit to our non-normalized gradient dictionary and yields coherence-based recovery guarantees and robustness (impossibility) certificates for K -flip budgets. Experiments on synthetic dictionaries and the Stanford Human Preferences dataset validate the theory and highlight how dictionary geometry governs attack success.

1. Introduction

Reinforcement learning from human feedback (RLHF) is a popular approach for aligning a learned policy with human preferences when an explicit reward function is hard to specify (Christiano et al., 2017; Casper et al., 2023). In many practical pipelines, the policy is trained from a pre-collected dataset of pairwise preference labels (Christiano et al., 2017;

Bai et al., 2022; Rafailov et al., 2023), which is referred to as *offline* RLHF (Xiong et al., 2023), to differentiate it from *online* RLHF where the policy is learned from real-time interactions with human feedbacks (Wang et al., 2023). Recent work has demonstrated that RLHF faces substantial security issues related to the reliability of the human preference data, i.e., when there are adversarial attacks on preferences or random noises in human preferences (Casper et al., 2023). The preference data can be manipulated by adversaries to mislead both offline and online RLHF to produce targeted outcomes (Wu et al., 2024a; Fu et al., 2025; Baumgärtner et al., 2024; Nika et al., 2025; Pathmanathan et al., 2025; Yang et al., 2025).

Two types of adversarial attack models are commonly studied in offline RLHF (Rando & Tramèr, 2023; Wu et al., 2024a; Baumgärtner et al., 2024; Nika et al., 2025): (i) label flip attack, which flips some labels within the original dataset; and (ii) data injection attack, which appends poisoned trajectories and preferences to the original dataset. In particular, (Rando & Tramèr, 2023; Wu et al., 2024a; Baumgärtner et al., 2024) provide valuable experimental results on the impact of label flip and data injection attacks, but focus less on the theoretical analysis. (Nika et al., 2025) provides a comprehensive theoretical analysis of the effectiveness of data injection attacks, showing that to mislead offline RLHF, the attacker needs to append numerous poisoned preference pairs, with size scaling linearly with the original dataset.

However, while label flip attacks on offline RLHF is practically plausible, a comprehensive theoretical study of such a setup remains an open problem. We aim to address this critical gap in this paper. Understanding this vulnerability is crucial for developing robust algorithms and ensuring the reliability of RLHF systems in real-world applications, e.g., designing helpful and harmless LLMs robust to adversarial attacks on training set. Compared with the data injection attack, the problem of understanding label flipping attack is more challenging: First, flips are limited to the original dataset: the attacker can only change labels on existing comparisons and cannot freely create arbitrary many new preference pairs. Second, the effect of flipping a single label on the learned policy is hard to predict, which makes it difficult to effectively choose which labels to attack.

¹Department of Electrical and Computer Engineering, University of California, Davis, Davis, CA, USA ²Department of Electrical and Computer Engineering, University of Iowa, Iowa City, IA, USA. Correspondence to: Chenye Yang <cyyyang@ucdavis.edu>, Weiyu Xu <weiyu-xu@uiowa.edu>, Lifeng Lai <lflai@ucdavis.edu>.

To our best knowledge, this work is the first to provide a theoretical analysis of *label flip* attacks on offline RLHF, specifically on Direct Preference Optimization (DPO) pipeline (Rafailov et al., 2023) under the log-linear policy class. Our focus on log-linear policies follows prior RLHF theory (Xiong et al., 2023; Chowdhury et al., 2024; Nika et al., 2025) and isolates the core geometric phenomenon that drives flip attacks. The main technical observation is simple but powerful: in log-linear DPO, flipping one preference label changes the gradient of the DPO objective by a vector that does not depend on the current policy parameter. The attacker’s problem can therefore be expressed in *gradient space* as selecting a subset of existing preference pairs whose flip-induced gradient shifts add up to (or closely approximate) a target vector, which is decided by the attacker’s desired policy to force the learner to adopt. We further show that controlling the gradient residual is a sufficient surrogate for policy-space attack success.

The reduction above implies that finding the optimal targeted flip attacks is a combinatorial problem and, in general, is computationally hard. To address this, we develop two algorithms with different focuses. First, for the general minimum-flip objective, we propose a *Binary-Aware Lattice Attack* (BAL-A). BAL-A uses a lattice embedding that simultaneously penalizes residual error and non-binary coefficients, and then applies Lenstra-Lenstra-Lovász (LLL) basis reduction and Babai’s nearest-plane algorithm to produce an integer solution that can be interpreted as a flip pattern. We further analyze how the embedding parameter controls the method and show that sufficiently large penalty enforces small integer coefficients and the proposed method finds the true minimum-flip solution under a separation condition. Second, when the attacker has a flip budget K and the true attack is sparse, we propose *Binary Matching Pursuit Attack* (BMP-A), a greedy method adapted from Binary Matching Pursuit (Wen & Li, 2021). BMP-A selects examples using normalized correlations to handle non-normalized gradient columns and admits coherence-based recovery guarantees. We also provide simple robustness certificates showing when *no* K -flip attack can succeed.

We validate the theory on synthetic dictionaries and on dictionaries constructed from the Stanford Human Preferences (SHP) dataset (Ethayarajh et al., 2022). The synthetic setting allows controlled tests of the lattice penalty and the coherence conditions. On SHP, we observe that BAL-A’s success depends sharply on the penalty region predicted by the separation analysis, and that BMP-A benefits substantially from reducing dictionary coherence, supporting our theoretical results.

Additional Related Work: Adversarial attacks on bandit and standard RL problems have been extensively studied. In these setups, the attacker manipulates rewards, actions, and

transitions to force the learner toward targeted behaviors. However, attacks on RLHF changes *human feedback*, such as preference labels, which are discrete, and indirectly shape the learned policy, making the effect of a single corruption harder to analyze. We summarize these additional related work in Appendix A.

2. Problem Formulation

2.1. Offline RLHF and DPO

In offline RLHF, we observe a fixed dataset \mathcal{D} consisting of pairwise preferences over two candidate actions/responses a under the same state/prompt s . We write each comparison as (s, a, a', o) , where $o \in \{+1, -1\}$ encodes which action is preferred by the human labeler. $o = +1$ means $a \succ a'$, while $o = -1$ means $a' \succ a$. Given a reference policy μ with parameter θ_μ , Direct Preference Optimization (DPO) trains a parametric policy π_θ directly from these comparisons, without explicitly fitting a reward model (Rafailov et al., 2023).

We focus on the log-linear policies for DPO, as defined in Definition 2.1. Log-linear policy class is commonly considered in RLHF literature (Xiong et al., 2023; Chowdhury et al., 2024; Nika et al., 2025), and it features many good properties in the further analysis.

Definition 2.1 (Log-linear Policy (Nika et al., 2025)). Let ψ be a d -dimensional feature mapping $\psi : \mathcal{S} \times \mathcal{A} \rightarrow \mathbb{R}^d$ with $\max_{s,a} \|\psi(s, a)\| \leq 1$. We consider the following class of log-linear policies $\forall (s, a) \in \mathcal{S} \times \mathcal{A}$ where $\theta \in \mathbb{R}^d$:

$$\Pi^{\log} = \left\{ \pi_\theta : \pi_\theta(a | s) = \frac{\exp(\psi(s, a)^\top \theta)}{\sum_{a'} \exp(\psi(s, a')^\top \theta)} \right\}.$$

Then, the DPO objective can be written as a regularized logistic loss over comparisons (Rafailov et al., 2023):

$$L_{\text{DPO}}(\theta; \mathcal{D}) = - \sum_{(s, a, a', o) \in \mathcal{D}} \log \sigma \left(o \cdot \beta \left(\log \frac{\pi_\theta(a | s)}{\mu(a | s)} - \log \frac{\pi_\theta(a' | s)}{\mu(a' | s)} \right) \right) + \frac{\lambda}{2} \|\theta - \theta_\mu\|_2^2,$$

where $\sigma(\cdot)$ is the sigmoid function, $\beta > 0$ is a temperature parameter, and $\lambda > 0$ is the regularization parameter. For reader’s convenience, we summarize the main steps of the derivation of DPO from the RLHF pipeline provided in (Rafailov et al., 2023) in Appendix B.

2.2. Preference Attack

We study label flip attacks on offline preference datasets. The attacker selects a subset of comparisons and flips their outcomes, equivalently changing o_i to $-o_i$ on the chosen

indices. The size of the dataset is fixed. Let $x \in \{0, 1\}^n$ indicate which comparisons are flipped, and write $\tilde{\mathcal{D}}(x)$ as the attacked dataset.

In this paper, a targeted label flip attacker’s optimization problem is formulated as:

$$\min_{x \in \{0,1\}^n} \|x\|_0 \quad \text{s.t.} \quad \|\pi_{\hat{\theta}(\tilde{\mathcal{D}}(x))} - \pi^\dagger\|_1 \leq \varepsilon,$$

Here $\hat{\theta}(\tilde{\mathcal{D}}(x))$ is the DPO policy parameter trained on the attacked dataset, and $\pi_{\hat{\theta}(\tilde{\mathcal{D}}(x))}$ is the corresponding policy. In this formulation, the goal of the attacker is to force $\pi_{\hat{\theta}(\tilde{\mathcal{D}}(x))}$ to align with a target policy π^\dagger (with parameter θ^\dagger) decided by the attacker, while modifying as few labels as possible.

We also consider a budgeted variant, in which the attacker can at most flip K entries in the training dataset:

$$\min_{x \in \{0,1\}^n: \|x\|_0 \leq K} \|x\|_0 \quad \text{s.t.} \quad \|\pi_{\hat{\theta}(\tilde{\mathcal{D}}(x))} - \pi^\dagger\|_1 \leq \varepsilon,$$

3. Label Flip Attack on DPO

3.1. Effect of Label Flip Attack

The DPO optimization problem with log-linear policy can be written as $\min_{\theta} L_{\text{DPO}}(\theta; \mathcal{D})$. For sample i : (s_i, a_i, a'_i, o_i) , the per-sample loss is

$$\ell_i(\theta) = -\log \sigma \left(o_i \beta \left(\log \frac{\pi_{\theta}(a_i | s_i)}{\mu(a_i | s_i)} - \log \frac{\pi_{\theta}(a'_i | s_i)}{\mu(a'_i | s_i)} \right) \right). \quad (1)$$

Using (1), the overall DPO loss can be written as:

$$L_{\text{DPO}}(\theta; \mathcal{D}) = \sum_{j \in \mathcal{D}} \ell_j(\theta) + \frac{\lambda}{2} \|\theta - \theta_{\mu}\|^2.$$

Theorem 3.1 (Flip-induced gradient shift for log-linear DPO). *Fix a comparison (s_i, a_i, a'_i, o_i) with $o_i \in \{+1, -1\}$, and define the feature difference $\Delta\psi_i := \psi(s_i, a_i) - \psi(s_i, a'_i) \in \mathbb{R}^d$. Let $\ell_i(\theta)$ be the per-sample DPO loss in (1), and let $g_i(\theta) := \nabla_{\theta} \ell_i(\theta)$. If we flip the label o_i to $\tilde{o}_i = -o_i$, and we have $\tilde{g}_i(\theta)$ replacing the o_i with \tilde{o}_i in $g_i(\theta)$, then for every θ the per-sample gradient changes by a constant vector that is independent of θ :*

$$\Delta g_i := \tilde{g}_i(\theta) - g_i(\theta) = o_i \beta \Delta\psi_i.$$

Theorem 3.1 is the key structural property behind our attack formulation: each flipped comparison contributes a fixed “atom” in gradient space for all values of policy parameter θ .

3.2. Formulate Label Flip Attack Problem

Using Theorem 3.1, when the attacker flip a set $\mathcal{F} \subset \mathcal{D}$, the attacked gradient becomes:

$$\begin{aligned} \nabla_{\theta} L_{\text{DPO}}(\theta; \tilde{\mathcal{D}}) &= \sum_{j \notin \mathcal{F}} g_j(\theta) + \sum_{i \in \mathcal{F}} \tilde{g}_i(\theta) + \lambda(\theta - \theta_{\mu}) \\ &= \nabla_{\theta} L_{\text{DPO}}(\theta; \mathcal{D}) + \Delta g_{\mathcal{F}}, \end{aligned}$$

where $\Delta g_{\mathcal{F}} := \sum_{i \in \mathcal{F}} \Delta g_i$ is a term depending on \mathcal{F} , but not on θ . Strong convexity of $L_{\text{DPO}}(\theta; \tilde{\mathcal{D}})$ (Lemma E.14 (Nika et al., 2025)) ensures that the first order condition (FOC) is enough to guarantee optimality. Then FOC minimizer for the attacked problem, $\tilde{\theta}$, satisfies:

$$\nabla_{\theta} L_{\text{DPO}}(\tilde{\theta}; \tilde{\mathcal{D}}) = \nabla_{\theta} L_{\text{DPO}}(\tilde{\theta}; \mathcal{D}) + \Delta g_{\mathcal{F}} = 0.$$

Now we need to study: if we want the learned policy $\tilde{\theta}$ to be some (target) policy θ^\dagger , what should the set \mathcal{F} be?

From the FOC above, we have:

$$g^\dagger := \nabla_{\theta} L_{\text{DPO}}(\theta^\dagger; \mathcal{D}) = -\Delta g_{\mathcal{F}} = -\sum_{i \in \mathcal{F}} o_i \beta \Delta\psi_i,$$

where we define g^\dagger as the gradient of the clean DPO loss at the target θ^\dagger .

For simplicity, denote $v_i = o_i \beta \Delta\psi_i$, $V = [v_1, \dots, v_n] \in \mathbb{R}^{d \times n}$. Then the label flip attack problem becomes:

$$\min_{\mathcal{F}} |\mathcal{F}| \quad \text{s.t.} \quad \sum_{i \in \mathcal{F}} v_i = -g^\dagger.$$

It can be seen as a binary sparse approximation problem:

$$\min_{x \in \{0,1\}^n} \mathbf{1}^\top x \quad \text{s.t.} \quad Vx = -g^\dagger.$$

We note that, in the label flip attack problem, the matrix V is fixed and determined by the original dataset \mathcal{D} , and the target gradient $-g^\dagger$ is also fixed and determined by the target policy θ^\dagger . The vector x is a binary vector indicating which samples to flip in the dataset \mathcal{D} .

When we allow some approximation error ε in reaching the target policy θ^\dagger , we say that: a flip attack is *exactly successful* if $Vx + g^\dagger = 0$, and *approximately successful* if $\|Vx + g^\dagger\|_2 \leq \varepsilon$. Thus, the exact and approximate flip attack problems can be written as:

$$\min_{x \in \{0,1\}^n} \mathbf{1}^\top x \quad \text{s.t.} \quad Vx + g^\dagger = 0, \quad (2)$$

and

$$\min_{x \in \{0,1\}^n} \mathbf{1}^\top x \quad \text{s.t.} \quad \|Vx + g^\dagger\|_2 \leq \varepsilon. \quad (3)$$

3.3. From Gradient Residual to Policy Closeness

For log-linear policies, prior work justifies treating a *parameter-space* target as a surrogate for a *policy-space* success criterion. In particular, Lemma E.5 of (Nika et al., 2025) relate an ℓ_1 policy-closeness constraint with tolerance ϵ to a parameter-closeness constraint with tolerance ϵ' : when $\epsilon' \leq \epsilon/(2\sqrt{d})$, parameter feasibility implies policy feasibility, and they also provide conditions for the reverse implication. Motivated by this equivalence, we analyze poisoning around a target parameter θ^\dagger and connect attack success to how flips perturb the DPO optimality conditions.

By construction,

$$\nabla_{\theta} L_{\text{DPO}}(\theta^\dagger; \tilde{\mathcal{D}}) = \nabla_{\theta} L_{\text{DPO}}(\theta^\dagger; \mathcal{D}) + Vx = g^\dagger + Vx. \quad (4)$$

Hence, the approximate flip-attack constraint

$$\|Vx + g^\dagger\|_2 \leq \varepsilon \quad (5)$$

is exactly a bound on the *gradient residual* at θ^\dagger for the poisoned objective, i.e., it enforces that θ^\dagger is an ε -stationary point of $L_{\text{DPO}}(\cdot; \tilde{\mathcal{D}})$. The following lemma shows that, under strong convexity, such approximate stationarity guarantees that training on $\tilde{\mathcal{D}}$ produces a parameter (and thus a policy) close to the target.

Lemma 3.2 (Gradient residual to policy closeness). *Assume $L_{\text{DPO}}(\cdot; \tilde{\mathcal{D}})$ is differentiable and μ -strongly convex in θ , e.g., for log-linear DPO with ℓ_2 regularization, see (Nika et al., 2025). Let $\hat{\theta} := \arg \min_{\theta} L_{\text{DPO}}(\theta; \tilde{\mathcal{D}})$ and define the trained policy $\pi_{\hat{\theta}, \tilde{\mathcal{D}}} := \pi_{\hat{\theta}}$, with target policy $\pi^\dagger := \pi_{\theta^\dagger}$. If $\|Vx + g^\dagger\|_2 \leq \varepsilon$ holds, equivalently $\|\nabla_{\theta} L_{\text{DPO}}(\theta^\dagger; \tilde{\mathcal{D}})\|_2 \leq \varepsilon$, then*

$$\|\hat{\theta} - \theta^\dagger\|_2 \leq \varepsilon/\mu. \quad (6)$$

Moreover, for log-linear policies this parameter bound implies the policy-space guarantee $\|\pi_{\hat{\theta}} - \pi^\dagger\|_1 \leq \epsilon$ whenever $\varepsilon \leq \mu \epsilon/(2\sqrt{d})$.

Lemma 3.2 justifies (5) as a sufficient condition for approximate attack success in policy space. This motivates our focus on the gradient perturbation at θ^\dagger ; in the log-linear DPO case, the per-example flip induces a parameter-independent gradient shift, yielding a fixed dictionary of vectors (the columns of V) and the binary selection formulation developed before.

3.4. Feasibility of Label Flip Attack

The feasibility question asks whether there exists $x \in \{0, 1\}^n$ such that $\|Vx + g^\dagger\|_2 \leq R$, where $R = 0$ for (2) and $R = \varepsilon$ for (3). This decision problem is NP-hard in general. Equivalently, feasibility means that $-g^\dagger$ lies within distance R of the finite attainable set $\mathcal{A} := \{Vx : x \in \{0, 1\}^n\}$.

Therefore, we assume in the following that a feasible flip attack exists as in Assumption 3.3, and focus on finding the

attack set \mathcal{F} and quantifying the cost of such an attack in terms of the number of flipped labels $|\mathcal{F}|$.

Assumption 3.3 (Existence of feasible flip attack). There exists a *true* binary attack vector $x^* \in \{0, 1\}^n$ such that $\|Vx^* + g^\dagger\|_2 \leq R$. In the exact problem we take $R = 0$, and in the approximate problem we take $R = \varepsilon$.

3.5. Lower-bound of Flips

We now derive a simple lower bound on the number of flipped labels $|\mathcal{F}|$ required for a successful flipping attack.

Theorem 3.4 (Norm-based lower-bound of $|\mathcal{F}|$). *If the attacker achieves the exact constraint in the exact problem (2), then the number of flips ($|\mathcal{F}|$ or $\mathbf{1}^\top x$) must satisfy $|\mathcal{F}| \geq \|g^\dagger\|_2/(2\beta)$. If the attacker is allowed tolerance $\varepsilon \geq 0$ and achieves the constraint in the approximate problem (3), then the number of flips must satisfy $|\mathcal{F}| \geq (\|g^\dagger\|_2 - \varepsilon)/(2\beta)$.*

Theorem 3.4 shows that, the number of flips must grow at least linearly with the norm of the target gradient $\|g^\dagger\|_2$. The bounds do not require any structural assumptions on the attack matrix V beyond the feature norm bound from Definition 2.1. They provide a simple necessary condition on $|\mathcal{F}|$ under the Assumption 3.3 of a feasible flip attack.

4. Binary-Aware Lattice Attack (BAL-A)

In this section, we discuss why a standard lattice formulation for the closest vector problem (CVP) can not handle the flip attack problem, even they are similar. Motivated by the limitations, we introduce a *binary-aware* lattice embedding combined with Babai’s nearest-plane algorithm. We derive sufficient conditions under which the result is guaranteed to be binary and recover the minimum-flip.

4.1. Lattice Method and a Binary-aware Embedding

The exact flip attack is the minimum-flip feasibility problem:

$$\min_{x \in \{0, 1\}^n} \mathbf{1}^\top x \quad \text{s.t.} \quad Vx + g^\dagger = 0. \quad (7)$$

A common approximate relaxation approach replaces the hard constraint by residual minimization, which, however, results in a different objective:

$$\min_{x \in \{0, 1\}^n} \|Vx + g^\dagger\|_2. \quad (8)$$

A natural relaxation of (8) is to allow integer coefficients,

$$\min_{z \in \mathbb{Z}^n} \|Vz + g^\dagger\|_2, \quad (9)$$

and view this as a CVP in the lattice (Lenstra et al., 1982) $L := \{Vz : z \in \mathbb{Z}^n\} \subset \mathbb{R}^d$ with target $t := -g^\dagger$. Indeed, $\text{dist}(L, t) := \min_{z \in \mathbb{Z}^n} \|Vz - t\|_2 = \min_{z \in \mathbb{Z}^n} \|Vz + g^\dagger\|_2$

$g^\dagger\|_2$. One can then apply lattice basis reduction (e.g., LLL (Lenstra et al., 1982)) and Babai’s nearest-plane algorithm (Babai, 1986) to obtain an integer vector $z \in \mathbb{Z}^n$ that approximately solves (9).

The lattice relaxation (9) is a natural starting point, but it does not directly match the binary minimum-flip model (7) in two key ways: binary coefficients, and minimum-flip objective. We summarize the mismatches in Appendix C.

These issues motivate a different design: rather than solving an unrestricted integer problem and truncating afterwards, we construct a *binary-aware* lattice embedding where non-binary coefficients are heavily penalized in the lattice norm, so that any sufficiently short lattice vector must already correspond to a (near) binary solution.

We work directly with the real-valued attack matrix V and gradient g^\dagger . Assume that the flip-effect vectors are uniformly bounded $\|v_i\|_2 \leq B$ ($B = 2\beta$, shown in Appendix J.3), we build a lattice in \mathbb{R}^{d+n} using the $(d+n) \times (n+1)$ real basis

$$B_{\text{bin}} := \begin{pmatrix} V & -g^\dagger \\ MI_n & 0 \end{pmatrix}, \quad M > 0,$$

whose columns are $b_i = (v_i; Me_i)$ for $i = 1, \dots, n$ and $b_{n+1} = (-g^\dagger; 0)$. For any integer vector $z \in \mathbb{Z}^n$, consider the coefficient vector $u(z) := (z; -1) \in \mathbb{Z}^{n+1}$, and the corresponding lattice vector

$$y(z) := B_{\text{bin}} u(z) = \begin{pmatrix} Vz + g^\dagger \\ Mz \end{pmatrix} \in \mathbb{R}^{d+n}.$$

Its squared norm decomposes as

$$\|y(z)\|_2^2 = \|Vz + g^\dagger\|_2^2 + M^2\|z\|_2^2. \quad (10)$$

Intuitively, the top block of B_{bin} measures how well z approximates the target $-g^\dagger$ (attack effectiveness), while the bottom block penalizes the magnitude of the coefficients z_i . Thus, choosing M sufficiently large discourages non-physical solutions with $|z_i| \geq 2$, addressing the second mismatch above. Moreover, for binary flip indicators $x \in \{0, 1\}^n$ we have $\|x\|_2^2 = \mathbf{1}^\top x$, so restricting (10) to binary vectors yields

$$\min_{x \in \{0, 1\}^n} \|Vx + g^\dagger\|_2^2 + M^2 \mathbf{1}^\top x, \quad (11)$$

which couples residual minimization with the flip count and hence address the first mismatch. In particular, on the feasible set $\{x \in \{0, 1\}^n : Vx + g^\dagger = 0\}$ the residual term vanishes and (11) reduces to minimizing $\mathbf{1}^\top x$; therefore, whenever an exact attack is achievable, minimizing $\|y(x)\|_2$ over feasible binary solutions is equivalent to (2).

We summarize the practical attack method based on the binary-aware lattice embedding and Babai’s nearest-plane

in Algorithm 1, shown in Appendix D. The inputs are the dataset matrix $V \in \mathbb{R}^{d \times n}$, the target gradient $g^\dagger \in \mathbb{R}^d$, and a penalty parameter $M > 0$. The method first embeds the binary flip selection problem into a lattice by augmenting each column v_i with a scaled identity component Me_i , so that nearest-lattice decoding corresponds to minimizing the binary-aware objective $\|Vz + g^\dagger\|_2^2 + M^2\|z\|_2^2$ over integer vectors z . It then applies LLL reduction to obtain a better-conditioned basis and uses Babai’s nearest-plane rounding to recover an integer coefficient vector, which is mapped back to the original coordinates and then truncated to produce a candidate flip pattern. For completeness, we provide the full step-by-step procedure (including the LLL and Babai) in Appendix D.

4.2. Theoretical Guarantees for BAL-A

4.2.1. LARGE M ENFORCES BINARY COEFFICIENTS

We formalize how the penalty parameter M controls the integer coefficients in the binary-aware embedding.

Lemma 4.1 (Coefficient bound for the shortest binary-aware lattice vector). *Assume the flip-effect vectors are bounded as $\|v_i\|_2 \leq B$ for all i . Suppose there exists a binary flip attack $x^* \in \{0, 1\}^n$ with support size $K^* := \|x^*\|_0$ and residual $\|Vx^* + g^\dagger\|_2 \leq R$. Let $z^{\text{opt}} \in \arg \min_{z \in \mathbb{Z}^n} \|y(z)\|_2$ be any minimizer of the binary-aware lattice norm over \mathbb{Z}^n . Then there exists $M_0 = M_0(B, R, K^*)$ such that for all $M \geq M_0$, every coordinate satisfies $|z_i^{\text{opt}}| \leq 1$, i.e., $z^{\text{opt}} \in \{-1, 0, 1\}^n$. One explicit sufficient choice is*

$$M_0 = (B\sqrt{K^*} + \sqrt{B^2K^* + 6BR + 3B^2})/3. \quad (12)$$

Lemma 4.1 shows that if there exists a reasonably good binary attack $x^* \in \{0, 1\}^n$, then for a sufficiently large M the global minimizer of the embedded lattice norm over \mathbb{Z}^n cannot contain any coefficient with magnitude ≥ 2 .

Theorem 4.2 (Binary optimality under nonnegativity). *Under the assumptions of Lemma 4.1, assume additionally that we restrict to nonnegative coefficients, i.e., $z \in \mathbb{Z}_{\geq 0}^n$, which is natural when each v_i already encodes the flip direction. Let $z^{\text{opt}} \in \arg \min_{z \in \mathbb{Z}_{\geq 0}^n} \|y(z)\|_2$. If $M \geq M_0(B, R, K^*)$, then $z^{\text{opt}} \in \{0, 1\}^n$ and*

$$\begin{aligned} \|y(z^{\text{opt}})\|_2^2 &= \|Vz^{\text{opt}} + g^\dagger\|_2^2 + M^2\|z^{\text{opt}}\|_2^2 \\ &\leq \|y(x^*)\|_2^2 \leq R^2 + M^2K^*. \end{aligned}$$

Theorem 4.2 converts the coefficient bound from Lemma 4.1 into an actual $\{0, 1\}^n$ guarantee under the natural constraint $z \in \mathbb{Z}_{\geq 0}^n$. Thus, the optimizer of the penalized embedding is a valid flip attack, which addresses the third mismatch.

4.2.2. SMALL M RECOVERS MINIMUM-FLIP OBJECTIVE

We now analyze how M controls the recovery of the minimum-flip objective in our flip attack problem.

Theorem 4.3 (Minimum-residual recovers minimum-flip). *Assume the exact flip attack is feasible, and let $x^* \in \arg \min_{x \in \{0,1\}^n} \mathbf{1}^\top x$ s.t. $Vx + g^\dagger = 0$. Define $K^* := \mathbf{1}^\top x^*$. For each $k \in \{0, 1, \dots, K^* - 1\}$ define the best k -flip residual $\rho_k := \min_{x \in \{0,1\}^n: \mathbf{1}^\top x = k} \|Vx + g^\dagger\|_2$. Consider the binary-aware surrogate objective*

$$F_M(x) := \|Vx + g^\dagger\|_2^2 + M^2 \mathbf{1}^\top x, \quad x \in \{0, 1\}^n.$$

If M satisfies the separation condition

$$\rho_k^2 > M^2 (K^* - k) \quad \text{for all } k = 0, 1, \dots, K^* - 1, \quad (13)$$

then every minimizer of $\min_{x \in \{0,1\}^n} F_M(x)$ is an optimal exact attack pattern; in particular, any minimizer is feasible ($Vx + g^\dagger = 0$) and has $\mathbf{1}^\top x = K^*$.

Theorem 4.3 states that $F_M(x)$ recovers the minimum-flip in exact attack case if all under-budget patterns ($k < K^*$) satisfy separation condition, and any minimizer of F_M must be feasible and use exactly K^* flips. This can be seen by a counterexample that when $M \geq \|g^\dagger\|_2$, the zero-flip solution $x = 0$ achieves the smallest objective value than any feasible solution with at least one flip.

The surrogate objective F_M trades off two goals: reducing the residual $\|Vx + g^\dagger\|_2$ and promoting discrete binary coefficients. In general, these goals can conflict, so there is no single, universal choice of M that guarantees recovering a feasible minimum-flip attack pattern for all instances. Moreover, if M is chosen too large, the penalty can favor under-selection (too few flips) even when an exact solution exists. Formal counterexamples are given in Appendix E.

5. Binary Matching Pursuit Attack (BMP-A)

In this section, we introduce the attack budget constraint K and study the sparse K -flip attack model. Then the K -flip attack problem can be viewed as a sparse recovery problem with a binary constraint on the coefficients. We adapt the Binary Matching Pursuit (BMP) algorithm (Wen & Li, 2021) to our flip attack setting and further provide sufficient conditions under which no K -flip attack can succeed.

5.1. Sparse K -Flip Attack Model

Equivalent to the flip attack formulation in Section 3.4, we define the minimum number of flips required for approximate success as

$$K^* := \min_{x \in \{0,1\}^n} \mathbf{1}^\top x \quad \text{s.t.} \quad \|Vx + g^\dagger\|_2 \leq R, \quad (14)$$

and ask whether $K^* < \infty$ (i.e., whether the constraint set is nonempty). Problem (14) is a binary optimization problem and is NP-hard in general.

As in classical sparse recovery, our analysis assumes that there exists an underlying feasible sparse solution to the attack constraint.

Assumption 5.1 (Existence of a feasible K^* -flip attack). *There exists a true binary attack vector $x^* \in \{0, 1\}^n$ and an integer $K^* \geq 1$ such that $\|x^*\|_0 = K^*$ and $\|Vx^* + g^\dagger\|_2 \leq R$. In the exact problem we take $R = 0$, and in the approximate problem we take $R = \varepsilon$.*

In practice, an adversary is typically constrained to modify only a small fraction of the data. We therefore focus on the *sparse attack* regime, where K^* is small. This motivates a budgeted K -flip model: for a given budget $K \geq K^*$, we restrict attention to attacks with $\|x\|_0 \leq K$ and study (i) impossibility conditions under which no such sparse attack can succeed, and (ii) algorithmic recovery of a successful sparse attack when it exists. Formally, we assume

Assumption 5.2 (Sparse attack model). $\|x^*\|_0 \leq K$ (equivalently, $K^* \leq K$).

In this way, K simultaneously models the attacker’s budget and provides a robustness scale: larger K makes attacks easier, while small K may render attacks impossible.

5.2. BMP-A’s Connection to Sparse Recovery

Our sparse flip-attack formulation is closely related to classical sparse recovery / sparse approximation. In the standard sparse recovery model, one observes (Tropp & Gilbert, 2007; Wen & Li, 2021) $y = Ax^* + e$, where $A \in \mathbb{R}^{d \times n}$ is a dictionary (or sensing matrix), $x^* \in \mathbb{R}^n$ is K -sparse, and e models noise. The goal is to identify the sparse support (and possibly the coefficients) of x^* from y . A canonical greedy method is Orthogonal Matching Pursuit (OMP) (Tropp & Gilbert, 2007), which iteratively selects the column of A most correlated with the current residual and then updates the residual after incorporating the selected atom.

In our setting, the “measurement” vector is the attack target $y := -g^\dagger$, the dictionary is the per-sample gradient contribution matrix $A := V$, and the attack is to find a *sparse binary selector* $x \in \{0, 1\}^n$ such that $Vx \approx -g^\dagger$, i.e., y is approximated by a sum of a small number of columns of V . Compared with classical sparse recovery, our coefficients are constrained to be binary (fixed to +1 on the chosen support), so the main task is *support selection* rather than continuous coefficient estimation. This viewpoint motivates pursuit-style greedy solvers, leading to our Binary Matching Pursuit Attack (BMP-A) in Algorithm 2, shown in Appendix G.

In BMP-A, we adapt BMP (Wen & Li, 2021) to our setting

while keeping the algorithm expressed in terms of the original non-normalized columns v_i of V and a binary selection vector $x \in \{0, 1\}^n$. Starting from $r^0 = y$ and $x^0 = 0$, BMP-A greedily picks one *unselected* index using the normalized score $|\langle v_i, r \rangle| / \|v_i\|_2$ per iteration and updates the residual by subtracting the selected *original* column $r \leftarrow r - v_{i_t}$. It stops after K iterations when the budget is exhausted, or when the residual is small $\|r\|_2 \leq \varepsilon$.

Most sparse-recovery analyses, including those for BMP (Wen & Li, 2021), assume that the dictionary columns are normalized to unit ℓ_2 -norm. In our problem, the columns v_i of V need not satisfy $\|v_i\|_2 = 1$, so BMP-A selects indices using *normalized* correlations. Define

$$a_i := \|v_i\|_2 > 0, \quad u_i := \frac{v_i}{a_i},$$

$$D := \text{diag}(a_1, \dots, a_n), \quad U := [u_1, \dots, u_n] = VD^{-1}.$$

Then for any binary attack $x \in \{0, 1\}^n$, we have $Vx = Uz$ with $z := Dx$, so z is K -sparse and has the *same support* as x , but with nonzero amplitudes $\{a_i : x_i = 1\}$ rather than 1. This normalization explains the BMP-A selection rule: at each step, $i_t \in \arg \max_{i \in [n] \setminus \Gamma} \frac{|\langle v_i, r \rangle|}{\|v_i\|_2} = \arg \max_{i \in [n] \setminus \Gamma} |\langle u_i, r \rangle|$, which is the standard correlation criterion under the unit-norm dictionary U . Likewise, mutual coherence is naturally defined using normalized directions,

$$\mu(V) := \max_{i \neq j} \frac{|\langle v_i, v_j \rangle|}{\|v_i\|_2 \|v_j\|_2} = \max_{i \neq j} |\langle u_i, u_j \rangle|.$$

Note, however, that passing from (V, x) to (U, z) changes the nonzero magnitudes from 1 to a_i ; consequently, recovery guarantees stated for unit-norm dictionaries with equal-magnitude nonzeros require a mild adjustment that depends on the column-norm ratio.

5.3. Theoretical Guarantees for BMP-A

5.3.1. RECOVERY OF x^* WITHIN BUDGET K

Under standard binary sparse-recovery conditions, we specially adapt the following guarantees to our setting.

Theorem 5.3 (Recovery under coherence). *Under the K^* -flip Assumption 5.1. Let $\mu(V)$ be defined as above and $b := \min_{1 \leq i \leq n} \|v_i\|_2$, $B := \max_{1 \leq i \leq n} \|v_i\|_2$. If*

$$\mu(V) < \frac{b}{(2K^* - 1)B} \quad (15)$$

and

$$\varepsilon < (b - (2K^* - 1)\mu(V)B)/2, \quad (16)$$

then BMP-A (Algorithm 2), selects an index in $\text{supp}(x^*)$ at each iteration. Consequently, after K^* iterations it exactly recovers $\text{supp}(x^*)$ and returns a binary vector \hat{x} with

$\text{supp}(\hat{x}) = \text{supp}(x^*)$. Moreover, once the correct support has been selected, $r^{K^*} = y - V\hat{x} = y - Vx^* = e$, so the stopping rule $\|r\|_2 \leq \varepsilon$ triggers no later than iteration K^* .

Theorem 5.3 is the direct analog of the coherence condition in (Wen & Li, 2021), but adapted to non-normalized columns through the norm range $b \leq \|v_i\|_2 \leq B$. Let $\rho := B/b$, the mutual coherence requirement scales as $\mu(V) \lesssim \frac{1}{(2K^* - 1)\rho}$: highly non-uniform column norms (large ρ) make recovery more stringent. When $b = B$, e.g., after normalization, (15)–(16) reduce to the standard guarantee of (Wen & Li, 2021).

5.3.2. IMPOSSIBILITY CONDITIONS FOR K -FLIP ATTACK

We now give sufficient conditions under which *no* K -flip attack can succeed, independent of specific attack algorithms.

Theorem 5.4 (Spectral norm and coherence impossibility). *Let $B := \max_i \|v_i\|_2$, $\mu(V)$ be defined as above, and $\|V\|_2$ be the spectral norm of V . Fix a budget $K \geq 1$ and tolerance $\varepsilon \geq 0$. If*

$$\|g^\dagger\|_2 - \varepsilon > \sqrt{K}\|V\|_2, \quad (17)$$

or

$$(\|g^\dagger\|_2 - \varepsilon)^2 > B^2(K + \mu(V)K(K - 1)), \quad (18)$$

then there does not exist any $x \in \{0, 1\}^n$ with $\|x\|_0 \leq K$ such that $\|Vx + g^\dagger\|_2 \leq \varepsilon$. In particular, (17) is a spectral-norm certificate, while (18) is a coherence-based refinement.

Theorem 5.4 provides sufficient conditions under which a K -flip attacker cannot drive the gradient residual at θ^\dagger below ε . It shows that the success of any label flip attack is limited by the geometry and scale of the flip-effect dictionary V . The spectral-norm condition (17) is universal: it only depends on the global operator norm $\|V\|_2$ and scales as \sqrt{K} . The coherence condition (18) is more refined: it separates the per-example strength B from the directional similarity $\mu(V)$. When columns are weak (small B) and point in diverse directions (small $\mu(V)$), even the best choice of K flips cannot create a large enough shift to cancel g^\dagger . These are certificates of robustness of DPO: failing them does not imply an attack exists, but satisfying them rules out *all* K -flip attacks, independent of specific attack algorithms.

6. Experiments and Results

In this section, we evaluate the proposed methods on both synthetic and real preference datasets.

6.1. Setup

We construct experiments with a K^* -flip ground truth, following Assumption 3.3. We sample $x^* \in \{0, 1\}^n$ with

$\|x^*\|_0 = K^*$ and set the target vector as $t := Vx^* = -g^\dagger$, so the exact constraint is feasible by design. Given an output \hat{x} , we report support recovery against x^* , e.g., true positive rate (TPR), and the residual $\|V\hat{x} - t\|_2$.

For synthetic data, we construct synthetic V from normalized random Gaussian columns. To validate the BAL-A separation behavior, we use a dictionary with $V \in \mathbb{R}^{64 \times 20}$ and $K^* = 5$ and sweep the lattice penalty M over 25 log-spaced values; we apply LLL pre-reduction ($\delta = 0.75$) before Babai and run 200 Monte Carlo trials. To validate BMP-A in the sparse regime, we fix a single low-coherence dictionary $V \in \mathbb{R}^{200 \times 200}$ and sweep the true sparsity level K^* ; for each K^* we run 200 trials and run BMP-A for exactly K^* iterations.

For real data, we construct V from the Stanford Human Preferences (SHP) dataset (Ethayarajh et al., 2022) by training a log-linear DPO model and forming the per-example flip-induced gradient shifts. For BAL-A, we use a smaller attacked subset ($n = 50$, $K^* = 7$) and sweep M . For BMP-A, we use a larger subset ($n = 401$, $K^* = 10$) and run BMP-A up to budget $K = 15$ with tolerance $\varepsilon = 10^{-3}$, comparing a random subset to a low-coherence subset of the same size. On SHP we use the same main metrics as in the synthetic experiments (support recovery and residual reduction), and we additionally report coherence statistics to highlight differences in dictionary geometry. We also compare the DPO model trained on attacked subset of SHP $\tilde{D}(\hat{x})$ to that trained on $\tilde{D}(x^*)$. Full setup details are deferred to Appendix H, and the SHP plots are deferred to Appendix I.

6.2. Results

6.2.1. VALIDATE BAL-A THEORY ON SYNTHETIC V

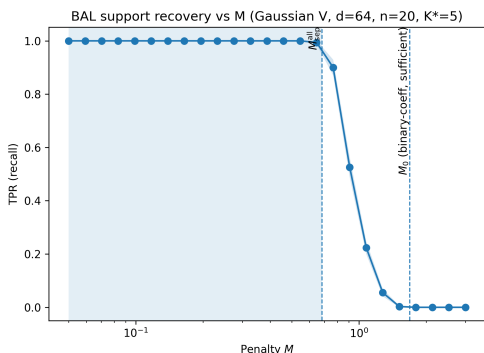


Figure 1. TPR of BAL-A on synthetic V as a function of M .

Figure 1 shows the support TPR of BAL-A as the lattice penalty M varies on a Gaussian synthetic dictionary. BAL-A recovers the true support almost perfectly for small M , but the recall drops quickly once M becomes moderately large. The transition happens around the separation thresh-

old $M_{\text{all sep}} \approx 0.68$ (vertical line) satisfying all of those in Theorem 4.3: below this value all the separation conditions hold and recovery is stable, while above it BAL-A increasingly miss the true flips. The binary-coefficient sufficient bound $M_0 \approx 1.69$ is overly conservative in this setting.

6.2.2. VALIDATE BMP-A THEORY ON SYNTHETIC V

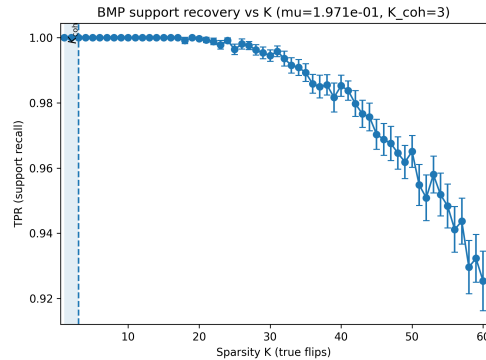


Figure 2. TPR of BMP-A on synthetic V as a function of K^* .

Figure 2 evaluates BMP-A on a fixed low-coherence synthetic dictionary while increasing the true number of flips K^* . The constructed matrix has empirical coherence $\mu(V) \approx 0.197$ and the corresponding guarantee in Theorem 5.3 only covers up to $K_{\text{coh}} = 3$ (vertical line). Within this guaranteed region, BMP-A achieves perfect support recovery. Beyond K_{coh} , the sufficient condition no longer applies, yet BMP-A still maintains high TPR and degrades gradually as K^* grows, indicating that the coherence bound is conservative in this synthetic setting and that BMP-A remains effective outside the sufficient guarantee.

6.2.3. RESULTS ON REAL DATA SET SHP

We also evaluate BAL-A and BMP-A on dictionaries constructed from the SHP dataset. Compared to the synthetic setting, SHP dictionaries are higher-dimensional (e.g., $d = 768$) and exhibit different geometry, including stronger correlations and non-uniform column norms. We report the same main metrics as in the synthetic experiments (support recovery and residual reduction), and for BMP-A we additionally compare a random subset to a low-coherence subset of the same size to isolate the role of dictionary coherence. We also report downstream diagnostics that compare the DPO model trained on the recovered flip set \hat{x} to that trained on the ground-truth flip set x^* . The SHP plots and detailed discussion are deferred to Appendix I.

7. Conclusion

We have studied label flip preference attacks on offline RLHF, specifically targeting the log-linear DPO pipeline.

We have illustrated the effect of flipping one preference label on the gradient of the DPO objective, and converted the attack problem to a binary sparse approximation problem in the per-sample gradient space. To solve it, we have proposed BAL-A algorithm, and provided sufficient conditions for binary coefficients and objective recovering. In practice, with budget K , we have also considered the K -flip attack problem and propose BMP-A, and provided a coherence-based recovery guarantee. We have also provided two impossibility conditions under which no K -flip attack can succeed. We have provided extensive experiments on both synthetic and real data to validate the theory.

Impact Statement

This paper presents work whose goal is to advance the field of Machine Learning. There are many potential societal consequences of our work, none which we feel must be specifically highlighted here.

References

- Abe, N., Biermann, A. W., and Long, P. M. Reinforcement learning with immediate rewards and linear hypotheses. *Algorithmica*, 37(4):263–293, 2003.
- Agarwal, A., Agarwal, S., and Patil, P. Stochastic dueling bandits with adversarial corruption. In *Proceedings of the International Conference on Algorithmic Learning Theory*, volume 132, pp. 217–248, Online, Mar. 2021.
- Auer, P. Using confidence bounds for exploitation-exploration trade-offs. *Journal of machine learning research*, 3(Nov):397–422, 2002.
- Auer, P., Cesa-Bianchi, N., Freund, Y., and Schapire, R. Gambling in a rigged casino: The adversarial multi-armed bandit problem. In *Proceedings of the IEEE Annual Foundations of Computer Science*, pp. 322–331, Milwaukee, WI, Oct. 1995.
- Auer, P., Cesa-Bianchi, N., Freund, Y., and Schapire, R. The nonstochastic multiarmed bandit problem. *SIAM Journal on Computing*, 32(1):48–77, 2002.
- Auer, P., Gajane, P., and Ortner, R. Adaptively tracking the best bandit arm with an unknown number of distribution changes. In *Proceedings of the Conference on Learning Theory*, volume 99, pp. 138–158, Phoenix, AZ, Jun. 2019.
- Babai, L. On lovász’ lattice reduction and the nearest lattice point problem. *Combinatorica*, 6(1):1–13, 1986.
- Bai, Y., Jones, A., Ndousse, K., Askell, A., Chen, A., Das-Sarma, N., Drain, D., Fort, S., Ganguli, D., Henighan, T., et al. Training a helpful and harmless assistant with reinforcement learning from human feedback. *arXiv preprint arXiv:2204.05862*, 2022.
- Banihashem, K., Singla, A., Gan, J., and Radanovic, G. Admissible policy teaching through reward design. In *Proceedings of the AAAI Conference on Artificial Intelligence*, volume 36, pp. 6037–6045, Online, Feb. 2022.
- Baumgärtner, T., Gao, Y., Alon, D., and Metzler, D. Best-of-venom: Attacking RLHF by injecting poisoned preference data. *arXiv preprint arXiv:2404.05530*, 2024.
- Besbes, O., Gur, Y., and Zeevi, A. Stochastic multi-armed-bandit problem with non-stationary rewards. In *Advances in Neural Information Processing Systems*, volume 27, Montréal, Canada, Dec. 2014.

- Besbes, O., Gur, Y., and Zeevi, A. Optimal exploration–exploitation in a multi-armed bandit problem with non-stationary rewards. *Stochastic Systems*, 9(4):319–337, 2019.
- Bradley, R. A. and Terry, M. E. Rank analysis of incomplete block designs: I. the method of paired comparisons. *Biometrika*, 39(3/4):324–345, 1952.
- Casper, S., Davies, X., Shi, C., Gilbert, T. K., Scheurer, J., Rando, J., Freedman, R., Korbak, T., Lindner, D., Freire, P., et al. Open problems and fundamental limitations of reinforcement learning from human feedback. *arXiv preprint arXiv:2307.15217*, 2023.
- Chen, X., Zhong, H., Yang, Z., Wang, Z., and Wang, L. Human-in-the-loop: Provably efficient preference-based reinforcement learning with general function approximation. In *Proceedings of the International Conference on Machine Learning*, volume 162, pp. 3773–3793, Baltimore, Maryland, Jul. 2022.
- Cheng, J., Xiong, G., Dai, X., Miao, Q., Lv, Y., and Wang, F.-Y. Rime: Robust preference-based reinforcement learning with noisy preferences. *arXiv preprint arXiv:2402.17257*, 2024.
- Cheung, W., Simchi-Levi, D., and Zhu, R. Hedging the drift: Learning to optimize under nonstationarity. *Management Science*, 68(3):1696–1713, 2022.
- Chowdhury, S. R., Kini, A., and Natarajan, N. Provably robust DPO: Aligning language models with noisy feedback. *arXiv preprint arXiv:2403.00409*, 2024.
- Christiano, P. F., Leike, J., Brown, T., Martic, M., Legg, S., and Amodei, D. Deep reinforcement learning from human preferences. *Advances in Neural Information Processing Systems*, 30:4302–4310, Dec. 2017.
- Ethayarajh, K., Choi, Y., and Swayamdipta, S. Understanding dataset difficulty with \mathcal{V} -usable information. In *Proceedings of the International Conference on Machine Learning*, volume 162, pp. 5988–6008, Baltimore, MD, Jul. 2022.
- Fu, T., Sharma, M., Torr, P., Cohen, S. B., Krueger, D., and Barez, F. Poisonbench: Assessing large language model vulnerability to data poisoning. *arXiv preprint arXiv:2410.08811*, 2025.
- Gajane, P., Urvoy, T., and Clérot, F. A relative exponential weighing algorithm for adversarial utility-based dueling bandits. In *Proceedings of the International Conference on Machine Learning*, volume 37, pp. 218–227, Lille, France, Jul. 2015.
- Garcelon, E., Roziere, B., Meunier, L., Tarbouriech, J., Teytaud, O., Lazaric, A., and Pirota, M. Adversarial attacks on linear contextual bandits. *Advances in Neural Information Processing Systems*, 33:14362–14373, 2020.
- Garivier, A. and Moulines, E. On upper-confidence bound policies for switching bandit problems. In *Proceedings of the International Conference on Algorithmic Learning Theory*, Espoo, Finland, Oct. 2011.
- Gleave, A., Dennis, M., Wild, C., Kant, N., Levine, S., and Russell, S. Adversarial policies: Attacking deep reinforcement learning. *arXiv preprint arXiv:1905.10615*, 2019.
- Huang, S., Papernot, N., Goodfellow, I., Duan, Y., and Abbeel, P. Adversarial attacks on neural network policies. *arXiv preprint arXiv:1702.02284*, 2017.
- Huang, Y. and Zhu, Q. Deceptive reinforcement learning under adversarial manipulations on cost signals. In *Proceedings of the International Conference on Decision and Game Theory for Security*, volume 10, pp. 217–237, Stockholm, Sweden, Oct. 2019.
- Jun, K.-S., Li, L., Ma, Y., and Zhu, X. Adversarial attacks on stochastic bandits. *Advances in Neural Information Processing Systems*, 31:3640–3649, Dec. 2018.
- Kos, J. and Song, D. Delving into adversarial attacks on deep policies. *arXiv preprint arXiv:1705.06452*, 2017.
- Lenstra, A. K., Lenstra, H. W., and Lovász, L. Factoring polynomials with rational coefficients. *Math. Ann.*, 261(4):515–534, 1982.
- Li, J., Zhang, B., Niu, Y., Wu, S., Ding, K., and Wu, J. Online reward poisoning in reinforcement learning with convergence guarantee. *IEEE Transactions on Information Forensics and Security*, 20:8891–8905, 2025.
- Li, L., Chu, W., Langford, J., and Schapire, R. E. A contextual-bandit approach to personalized news article recommendation. In *Proceedings of the International Conference on World Wide Web*, pp. 661–670, Raleigh, NC, Apr. 2010.
- Lin, Y.-C., Hong, Z.-W., Liao, Y.-H., Shih, M.-L., Liu, M.-Y., and Sun, M. Tactics of adversarial attack on deep reinforcement learning agents. *arXiv preprint arXiv:1703.06748*, 2017.
- Liu, F. and Shroff, N. Data poisoning attacks on stochastic bandits. In *Proceedings of the International Conference on Machine Learning*, volume 97, pp. 4042–4050, Long Beach, CA, Jun. 2019.

- Liu, G. and Lai, L. Action-manipulation attacks against stochastic bandits: Attacks and defense. *IEEE Transactions on Signal Processing*, 68:5152–5165, 2020.
- Liu, G. and Lai, L. Efficient action poisoning attacks on linear contextual bandits. *arXiv preprint arXiv:2112.05367*, 2021a.
- Liu, G. and Lai, L. Provably efficient black-box action poisoning attacks against reinforcement learning. *Advances in Neural Information Processing Systems*, 34:12400–12410, Dec. 2021b.
- Liu, G. and Lai, L. Efficient adversarial attacks on online multi-agent reinforcement learning. *Advances in Neural Information Processing Systems*, 36:24401–24433, Dec. 2023.
- Ma, E., Etesami, S. R., and Rathi, P. Reward poisoning on federated reinforcement learning. *Transactions on Machine Learning Research*, 2024. ISSN 2835-8856.
- Ma, Y. and Zhou, Z. Adversarial attacks on adversarial bandits. *arXiv preprint arXiv:2301.12595*, 2023.
- Ma, Y., Jun, K.-S., Li, L., and Zhu, X. Data poisoning attacks in contextual bandits. In *Proceedings of the International Conference on Decision and Game Theory for Security*, pp. 186–204, Seattle, WA, Oct. 2018.
- Ma, Y., Zhang, X., Sun, W., and Zhu, X. Policy poisoning in batch reinforcement learning and control. *Advances in Neural Information Processing Systems*, 32:14570–14580, Dec. 2019.
- Mandal, D., Nika, A., Kamalaruban, P., Singla, A., and Radanović, G. Corruption robust offline reinforcement learning with human feedback. *arXiv preprint arXiv:2402.06734*, 2024.
- Mandlekar, A., Zhu, Y., Garg, A., Fei-Fei, L., and Savarese, S. Adversarially robust policy learning: Active construction of physically-plausible perturbations. In *Proceedings of the IEEE/RSJ International Conference on Intelligent Robots and Systems*, pp. 3932–3939, Vancouver, Canada, Sep. 2017.
- McMahan, J., Wu, Y., Zhu, X., and Xie, Q. Optimal attack and defense for reinforcement learning. In *Proceedings of the AAAI Conference on Artificial Intelligence*, volume 38, pp. 14332–14340, Vancouver, Canada, Feb. 2024.
- Nika, A., Nöther, J., Mandal, D., Kamalaruban, P., Singla, A., and Radanovic, G. Policy teaching via data poisoning in learning from human preferences. In *Proceedings of the International Conference on Artificial Intelligence and Statistics*, Mai Khao, Thailand, May. 2025.
- Ouyang, L., Wu, J., Jiang, X., Almeida, D., Wainwright, C., Mishkin, P., Zhang, C., Agarwal, S., Slama, K., Ray, A., et al. Training language models to follow instructions with human feedback. *Advances in Neural Information Processing Systems*, 35:27730–27744, Nov. 2022.
- Pan, X., Xiao, C., He, W., Yang, S., Peng, J., Sun, M., Yi, J., Yang, Z., Liu, M., Li, B., et al. Characterizing attacks on deep reinforcement learning. *arXiv preprint arXiv:1907.09470*, 2019.
- Pathmanathan, P., Chakraborty, S., Liu, X., Liang, Y., and Huang, F. Is poisoning a real threat to LLM alignment? maybe more so than you think. *arXiv preprint arXiv:2406.12091*, 2024.
- Pathmanathan, P., Chakrabortya, S., Liu, X., Liang, Y., and Huang, F. Is poisoning a real threat to DPO? maybe more so than you think. In *Proceedings of the AAAI Conference on Artificial Intelligence*, volume 39, pp. 27556–27564, Philadelphia, PA, Feb. 2025.
- Pattanaik, A., Tang, Z., Liu, S., Bommannan, G., and Chowdhary, G. Robust deep reinforcement learning with adversarial attacks. *arXiv preprint arXiv:1712.03632*, 2017.
- Rafailov, R., Sharma, A., Mitchell, E., Manning, C. D., Ermon, S., and Finn, C. Direct preference optimization: Your language model is secretly a reward model. *Advances in Neural Information Processing Systems*, 36:53728–53741, Dec. 2023.
- Rakhsha, A., Radanovic, G., Devidze, R., Zhu, X., and Singla, A. Policy teaching via environment poisoning: Training-time adversarial attacks against reinforcement learning. In *Proceedings of International Conference on Machine Learning*, volume 119, pp. 7974–7984, Online, Jul. 2020.
- Rakhsha, A., Zhang, X., Zhu, X., and Singla, A. Reward poisoning in reinforcement learning: Attacks against unknown learners in unknown environments. *arXiv preprint arXiv:2102.08492*, 2021.
- Rando, J. and Tramèr, F. Universal jailbreak backdoors from poisoned human feedback. *arXiv preprint arXiv:2311.14455*, 2023.
- Rangi, A., Xu, H., Tran-Thanh, L., and Franceschetti, M. Understanding the limits of poisoning attacks in episodic reinforcement learning. *arXiv preprint arXiv:2208.13663*, 2022.
- Robbins, H. Some aspects of the sequential design of experiments. *Bulletin of the American Mathematical Society*, 58(5):527–535, September 1952.

- Saha, A., Koren, T., and Mansour, Y. Adversarial dueling bandits. In *Proceedings of the International Conference on Machine Learning*, volume 139, pp. 9235–9244, Online, Jul. 2021.
- Saha, A., Pacchiano, A., and Lee, J. Dueling RL: Reinforcement learning with trajectory preferences. In *Proceedings of the International Conference on Artificial Intelligence and Statistics*, volume 206, pp. 6263–6289, Valencia, Spain, Apr. 2023.
- Stephens-Davidowitz, N. Lattices mini course (NYU, Fall 2016): Lecture 5: CVP and Babai’s algorithm. Technical report, Computer Science Department, New York University, New York, NY, 2016.
- Sui, Y., Zoghi, M., Hofmann, K., and Yue, Y. Advances in dueling bandits. In *Proceedings of the International Joint Conference on Artificial Intelligence*, pp. 5502–5510, Stockholm, Sweden, Jul. 2018.
- Sun, J., Zhang, T., Xie, X., Ma, L., Zheng, Y., Chen, K., and Liu, Y. Stealthy and efficient adversarial attacks against deep reinforcement learning. In *Proceedings of the AAAI Conference on Artificial Intelligence*, volume 34, pp. 5883–5891, New York, NY, Feb. 2020a.
- Sun, Y., Huo, D., and Huang, F. Vulnerability-aware poisoning mechanism for online RL with unknown dynamics. *arXiv preprint arXiv:2009.00774*, 2020b.
- Tropp, J. A. and Gilbert, A. C. Signal recovery from random measurements via orthogonal matching pursuit. *IEEE Transactions on Information Theory*, 53(12):4655–4666, 2007.
- Wang, Y., Liu, Q., and Jin, C. Is RLHF more difficult than standard RL? a theoretical perspective. *Advances in Neural Information Processing Systems*, 36:76006–76032, 2023.
- Wen, J. and Li, H. Binary sparse signal recovery with binary matching pursuit. *Inverse Problems*, 37(6):065014, 2021.
- Wu, J., Wang, J., Xiao, C., Wang, C., Zhang, N., and Vorobeychik, Y. Preference poisoning attacks on reward model learning. *arXiv preprint arXiv:2402.01920*, 2024a.
- Wu, J., Xie, Y., Yang, Z., Wu, J., Chen, J., Gao, J., Ding, B., Wang, X., and He, X. Towards robust alignment of language models: Distributionally robustifying direct preference optimization. *arXiv preprint arXiv:2407.07880*, 2024b.
- Wu, J., Wang, J., Xiao, C., Wang, C., Zhang, N., and Vorobeychik, Y. Preference poisoning attacks on reward model learning. In *Proceedings of the IEEE Symposium on Security and Privacy*, pp. 1622–1640, San Francisco, CA, May. 2025.
- Wu, R. and Sun, W. Making RL with preference-based feedback efficient via randomization. *arXiv preprint arXiv:2310.14554*, 2024.
- Wu, Y., McMahan, J., Zhu, X., and Xie, Q. Reward poisoning attacks on offline multi-agent reinforcement learning. In *Proceedings of the AAAI Conference on Artificial Intelligence*, volume 37, pp. 10426–10434, Washington, DC, Feb. 2023.
- Xiong, W., Dong, H., Ye, C., Wang, Z., Zhong, H., Ji, H., Jiang, N., and Zhang, T. Iterative preference learning from human feedback: Bridging theory and practice for RLHF under KL-constraint. *arXiv preprint arXiv:2312.11456*, 2023.
- Xu, H., Wang, R., Raizman, L., and Rabinovich, Z. Transferable environment poisoning: Training-time attack on reinforcement learning. In *Proceedings of the International Conference on Autonomous Agents and Multiagent Systems*, pp. 1398–1406, Online, May. 2021.
- Xu, Y., Zeng, Q., and Singh, G. Efficient reward poisoning attacks on online deep reinforcement learning. *arXiv preprint arXiv:2205.14842*, 2022.
- Yan, Y., Lou, X., Li, J., Zhang, Y., Xie, J., Yu, C., Wang, Y., Yan, D., and Shen, Y. Reward-robust RLHF in LLMs. *arXiv preprint arXiv:2409.15360*, 2024.
- Yang, C., Liu, G., and Lai, L. Stochastic bandits with non-stationary rewards: Reward attack and defense. *IEEE Transactions on Signal Processing*, 72:5007–5020, 2024.
- Yang, C., Lyu, M., Liu, G., and Lai, L. Human feedback attack on online RLHF: Attack and robust defense. *IEEE Transactions on Signal Processing*, 73:3886–3901, 2025.
- Yue, Y., Broder, J., Kleinberg, R., and Joachims, T. The k-armed dueling bandits problem. *Journal of Computer and System Sciences*, 78(5):1538–1556, 2012.
- Zhan, W., Uehara, M., Sun, W., and Lee, J. D. Provable reward-agnostic preference-based reinforcement learning. *arXiv preprint arXiv:2305.18505*, 2023.
- Zhang, X., Ma, Y., Singla, A., and Zhu, X. Adaptive reward-poisoning attacks against reinforcement learning. In *Proceedings of the International Conference on Machine Learning*, volume 119, pp. 11225–11234, Online, Jul. 2020.
- Zhu, B., Jordan, M., and Jiao, J. Principled reinforcement learning with human feedback from pairwise or k-wise comparisons. In *Proceedings of the International Conference on Machine Learning*, volume 202, pp. 43037–43067, Honolulu, HI, Jul. 2023.

Zimmert, J. and Seldin, Y. An optimal algorithm for stochastic and adversarial bandits. In *Proceedings of the International Conference on Artificial Intelligence and Statistics*, volume 89, pp. 467–475, Okinawa, Japan, Apr. 2019.

Zoghi, M., Whiteson, S., Munos, R., and Rijke, M. Relative upper confidence bound for the k-armed dueling bandit problem. In *Proceedings of the International Conference on Machine Learning*, volume 32, pp. 10–18, Beijing, China, Jun. 2014.

A. Introduction: Additional Related Work

A.1. Adversarial Attacks on Bandits

A line of work has studied adversarial attacks on bandit problems, including multi-armed bandits (MAB) (Jun et al., 2018; Liu & Shroff, 2019; Liu & Lai, 2020; Ma & Zhou, 2023; Yang et al., 2024), linear contextual bandits (Ma et al., 2018; Garcelon et al., 2020; Liu & Lai, 2021a), and dueling bandits (Gajane et al., 2015; Agarwal et al., 2021; Saha et al., 2021). These works have demonstrated that bandit algorithms are vulnerable to adversarial manipulation.

In the MAB setting, the learner takes an action by selecting one arm each round and observes its reward (Robbins, 1952; Auer et al., 1995; 2002). An adversary can manipulate the reward signals to mislead the learning algorithm into selecting a target arm more frequently (Jun et al., 2018; Ma & Zhou, 2023; Liu & Shroff, 2019), or corrupt the action signals to influence the learning process (Liu & Lai, 2020). Most of these existing work focused on the stationary random rewards setting, in which the distribution of reward of each arm does not change over time. Some (Ma & Zhou, 2023) studied the adversarial setting, in which the reward given by the environment can be arbitrarily chosen (Auer et al., 2002; Zimmert & Seldin, 2019). Other work (Yang et al., 2024) considered non-stationary stochastic bandits, in which the reward distribution of each arm can change over time but with some constraints on the total amount of changes (Garivier & Moulines, 2011; Besbes et al., 2014; Auer et al., 2019; Besbes et al., 2019; Cheung et al., 2022).

In linear contextual bandits, the expected reward is modeled as a linear function of the context features (Auer, 2002; Abe et al., 2003; Li et al., 2010). Existing works on adversarial attacks against linear contextual bandits focus on the reward poisoning (Ma et al., 2018; Garcelon et al., 2020), where the attacker manipulates the reward signal; context poisoning (Garcelon et al., 2020), where the adversary modifies the context observed without changing the reward associated with the context; and action poisoning (Liu & Lai, 2021a), where the adversary changes the action selected by the learner.

In dueling bandits, the learner selects a pair of arms each round and observes relative feedback indicating which arm is preferred (Yue et al., 2012; Zoghi et al., 2014; Sui et al., 2018). Prior work studies stochastic dueling bandits with adversarial corruption, where an attacker can corrupt pairwise outcomes (Agarwal et al., 2021). Other works consider fully adversarial preference models, which can be viewed as an extreme form of corruption (Gajane et al., 2015; Saha et al., 2021).

A.2. Adversarial Attacks on Standard Reinforcement Learning

Adversarial attacks on standard reinforcement learning (RL) have been widely studied under different poisoning models, where the attacker modifies the learning signals to mislead the learned policy. Common corruptions include reward poisoning (manipulating reward or cost signals) (Huang & Zhu, 2019; Zhang et al., 2020; Rakhsha et al., 2020; 2021; Banihashem et al., 2022; Xu et al., 2022; Li et al., 2025), action poisoning (manipulating the agent’s action before it is applied) (Liu & Lai, 2021b), and more general environment poisoning such as manipulating transition dynamics (Rakhsha et al., 2020; Xu et al., 2021). Poisoning has also been studied in batch setting (Ma et al., 2019), and in dynamics-agnostic settings where attacker must learn to attack from interaction (Sun et al., 2020b; Liu & Lai, 2021b; Rakhsha et al., 2021; Xu et al., 2022; Li et al., 2025).

Beyond single-agent RL, adversarial attacks have been considered in more complex settings, including multi-agent RL where the attacker can corrupt rewards and/or actions (Liu & Lai, 2023; Wu et al., 2023), and federated RL where poisoning can exploit both the RL dynamics and the federated aggregation mechanism (Ma et al., 2024). There is also work that characterizes limits of reward-only or action-only poisoning in episodic RL (Rangi et al., 2022), as well as work that studies optimal attack in attacker’s Markov decision process (McMahan et al., 2024). In addition, many attacks are studied specifically in deep RL, where policies are neural networks and the attacker perturbs high-dimensional observations to induce harmful actions at decision time (Huang et al., 2017; Kos & Song, 2017; Lin et al., 2017; Pattanaik et al., 2017; Mandlekar et al., 2017; Pan et al., 2019; Gleave et al., 2019; Sun et al., 2020a),

A.3. Adversarial Attacks on Reinforcement Learning from Human Feedback

RLHF relies on human preference data as the training source, which is inherently different from bandit or standard RL settings that use numerical rewards. Recent works have shown that RLHF faces substantial security issues related to the reliability of preference data, i.e., when there are adversarial attacks on preferences or random noises in human preferences (Casper et al., 2023). In offline RLHF (Xiong et al., 2023), where the learner trains on a pre-collected preference dataset (Christiano et al., 2017; Ouyang et al., 2022; Bai et al., 2022; Zhu et al., 2023; Rafailov et al., 2023), preference data

can be manipulated by adversaries to mislead training and induce targeted behaviors (Wu et al., 2024a; Rando & Tramèr, 2023; Baumgärtner et al., 2024; Pathmanathan et al., 2024; Nika et al., 2025; Fu et al., 2025; Pathmanathan et al., 2025; Wu et al., 2025). Most existing studies demonstrate this vulnerability from data injection attacks and label flip attacks experimentally on large-scale models (Rando & Tramèr, 2023; Wu et al., 2024a; Baumgärtner et al., 2024; Pathmanathan et al., 2024; Fu et al., 2025; Pathmanathan et al., 2025; Wu et al., 2025), while (Nika et al., 2025) provides a comprehensive theoretical analysis of data injection attacks and shows that a large appended poisoned preference set may be needed to mislead offline RLHF. In online RLHF, where the agent learns from real-time interactions with human feedbacks (Chen et al., 2022; Saha et al., 2023; Wang et al., 2023; Zhan et al., 2023; Wu & Sun, 2024) adversaries also attack the preference to manipulate the learning process (Yang et al., 2025).

Besides adversarial poisoning, the preference data is also inherently noisy due to annotation difficulty, limited expert availability, and systematic differences across annotators (Casper et al., 2023; Yan et al., 2024). Such noise can lead to hard-to-predict behaviors and potential biases in aligned model outputs. Accordingly, a line of work studies robustness of offline RLHF under noisy or partially corrupted preferences (Yan et al., 2024; Cheng et al., 2024; Mandal et al., 2024; Chowdhury et al., 2024; Wu et al., 2024b). These works typically focus on random corruption models or random noise rather than a targeted adversarial attacker that strategically selects which comparisons to corrupt.

Compared with attacks on standard RL and bandits, attacks on RLHF face an additional challenge: the feedback is discrete preference data, and its effect on the learned policy is less direct and harder to predict. Moreover, in label flip attack problem for offline RLHF, the attacker is restricted to manipulating a fixed preference dataset, rather than freely manipulating rewards or transitions or generating new comparison pairs. Our work focuses on this practically plausible label flip threat model and provides a theoretical analysis for DPO under the log-linear policy class.

B. Problem Formulation: Offline RLHF Pipeline and DPO Derivation (Rafailov et al., 2023)

This appendix provides a short summary that connects the standard offline RLHF pipeline to the DPO objective used in the main paper. We note that these derivations were done in (Rafailov et al., 2023) with a slightly different notation. We include them here for readers’ convenience. The subsequent attack formulation and guarantees do not depend on the intermediate reward-modeling step.

RLHF frameworks usually combine three interconnected processes: feedback collection, reward modeling, and policy optimization (Christiano et al., 2017; Casper et al., 2023). Once given two answers a_1 and a_2 for the same prompt s , the human labeler is asked to compare the two answers and give their preference, denoted as $a_w \succ a_l \mid s$ where a_w is the preferred answer and a_l is the dispreferred answer in the pair (a_1, a_2) . Note that to match the notation in (Rafailov et al., 2023), this appendix writes each comparison as (s, a_w, a_l) , so the label is implicit. This is equivalent to the main-text notation (s, a, a', o) with $o \in \{+1, -1\}$ by setting

$$(a_w, a_l) = \begin{cases} (a, a'), & o = +1, \\ (a', a), & o = -1. \end{cases}$$

Equivalently, given (s, a_w, a_l) one can take $(s, a, a', o) = (s, a_w, a_l, +1)$.

We assume that there is some latent reward model $r^*(a, s)$ for the prompt s and the answer a , which can not be observed by anyone. Bradley-Terry model (Bradley & Terry, 1952) describes the human preference distribution p^* for pairwise comparisons:

$$p^*(a_1 \succ a_2 \mid s) = \frac{\exp(r^*(s, a_1))}{\exp(r^*(s, a_1)) + \exp(r^*(s, a_2))}.$$

In the offline RLHF setting, the agent has access to a static dataset of comparisons $\mathcal{D} = \{s^{(i)}, a_w^{(i)}, a_l^{(i)}\}_{i=1}^N$ sampled from p^* . Using the dataset \mathcal{D} , the agent can learn a reward model $r_\phi(s, a)$ parameterized by ϕ via maximum likelihood estimation (MLE). The negative log-likelihood loss function is defined as:

$$L_{\text{RLHF}}(r_\phi, \mathcal{D}) = -\mathbb{E}_{(s, a_w, a_l) \sim \mathcal{D}} [\log \sigma(r_\phi(s, a_w) - r_\phi(s, a_l))],$$

where $\sigma(x) = \frac{1}{1 + \exp(-x)}$ is the sigmoid function for the Bradley-Terry model. Then a RL algorithm is used to optimize a policy π_θ parameterized by θ with the learned reward model $r_\phi(s, a)$:

$$\max_{\pi_\theta} \mathbb{E}_{s \sim \mathcal{D}, a \sim \pi_\theta(a \mid s)} [r_\phi(s, a) - \beta \mathbb{D}_{\text{KL}}[\pi_\theta(a \mid s) \parallel \pi_{\text{ref}}(a \mid s)]],$$

where β is a parameter controlling the trade-off between learning the human preferences and following the reference policy π_{ref} .

To avoid the computational cost of policy optimization by reinforcement learning in large-scale problems, DPO (Rafailov et al., 2023) is proposed to directly optimize the policy π_θ with the preference data (s, a_w, a_l) . Solving the policy optimization problem leads to the following optimal solution:

$$\pi_r(a | s) = \frac{1}{Z(s)} \pi_{\text{ref}}(a | s) \exp\left(\frac{1}{\beta} r(s, a)\right),$$

where $Z(s) = \sum_a \pi_{\text{ref}}(a | s) \exp\left(\frac{1}{\beta} r(s, a)\right)$ is the partition function. Rearranging the above equation leads to:

$$r(s, a) = \beta \log \frac{\pi_r(a | s)}{\pi_{\text{ref}}(a | s)} + \beta \log Z(s).$$

Applying this reparameterization to the ground-truth reward function r^* and corresponding optimal policy π^* , and the Bradley-Terry model, we have:

$$p^*(a_1 \succ a_2 | s) = \frac{1}{1 + \exp\left(\beta \log \frac{\pi^*(a_2 | s)}{\pi_{\text{ref}}(a_2 | s)} - \beta \log \frac{\pi^*(a_1 | s)}{\pi_{\text{ref}}(a_1 | s)}\right)}.$$

In this way, we model the human preference probability as a function of the optimal policy π^* rather than the reward function r^* . Therefore, the loss function in MLE for parameterized policy π_θ can be rewritten as:

$$L_{\text{DPO}}(\pi_\theta; \pi_{\text{ref}}) = - \mathbb{E}_{(s, a_w, a_l) \sim \mathcal{D}} \left[\log \sigma \left(\beta \log \frac{\pi_\theta(a_w | s)}{\pi_{\text{ref}}(a_w | s)} - \beta \log \frac{\pi_\theta(a_l | s)}{\pi_{\text{ref}}(a_l | s)} \right) \right].$$

Solving this estimation problem leads to the desired policy π_θ .

C. BAL-A: Key Mismatches of the Standard Lattice Relaxation

This standard lattice approach has three key mismatches with our flip model:

1. **Objective mismatch (minimum residual vs. minimum flips).** The CVP-style formulation focuses on minimizing the residual $\min_{x \in \{0,1\}^n} \|Vx + g^\dagger\|_2$, whereas our flip attack is a *minimum-cardinality* problem: $\min_{x \in \{0,1\}^n} \mathbf{1}^\top x$. Even when an exact attack is feasible (so the residual is zero), residual minimization alone does not distinguish among multiple feasible solutions and therefore does not, in general, recover the minimum-flip pattern.
2. **Unbounded integer coefficients.** In (9), the coefficients z_i can be arbitrary integers, corresponding to “using” the same flip-effect v_i multiple times. In our setting, each data point can be flipped at most once, so the admissible coefficients must lie in $\{0, 1\}$. Large integer coefficients are not meaningful as physical flip patterns.
3. **No guaranteed truncation.** A common workaround is to truncate an integer solution to the binary hypercube, e.g., $x_i = \mathbf{1}\{z_i \geq 1\}$. This nonlinear projection can destroy the relationship between $\|Vz + g^\dagger\|_2$ and $\|Vx + g^\dagger\|_2$, and there is no guarantee that a near-optimal integer solution leads to a near-optimal binary solution.

D. BAL-A: Full Binary-Aware Lattice Attack Algorithm

The Binary-Aware Lattice Attack (BAL-A) algorithm is summarized in Algorithm 1.

Here we provide more details on each step of BAL-A:

1. **Construct the binary-aware lattice basis and target.**

(a) Form the extended basis

$$B_e = [b_1, \dots, b_n] \in \mathbb{R}^{(d+n) \times n}, \quad b_i := \begin{pmatrix} v_i \\ M e_i \end{pmatrix},$$

where $i = 1, \dots, n$ and e_i is the i -th standard basis vector in \mathbb{R}^n .

Algorithm 1 Binary-Aware Lattice Attack (BAL-A)

input $V = [v_1, \dots, v_n] \in \mathbb{R}^{d \times n}$, $g^\dagger \in \mathbb{R}^d$, $M > 0$, $\delta \in (1/4, 1)$

output $\hat{x} \in \{0, 1\}^n$

- 1: **Binary-aware Embedding:** $b_i := (v_i; Me_i)$, $B_e := [b_1, \dots, b_n]$, $t := (-g^\dagger; 0)$
- 2: **Basis Reduction:** $(\tilde{B}, T) \leftarrow \text{LLL}_\delta(B_e)$ with $\tilde{B} = B_e T$ (Lenstra et al., 1982)
- 3: **Nearest-plane:** $z \leftarrow \text{Babai}(\tilde{B}, t)$ (Babai, 1986)
- 4: $x_{\text{int}} \leftarrow Tz \in \mathbb{Z}^n$
- 5: **Truncation:** $\hat{x} \leftarrow \Pi_{\{0,1\}^n}(x_{\text{int}})$, i.e., $\hat{x}_i := \min\{1, \max\{0, x_{\text{int},i}\}\}$

- (b) Define the target vector

$$t := \begin{pmatrix} -g^\dagger \\ 0 \end{pmatrix} \in \mathbb{R}^{d+n}.$$

Minimizing $\|B_e x - t\|_2$ over $x \in \mathbb{Z}^n$ is equivalent to minimizing $\|Vx + g^\dagger\|_2^2 + M^2\|x\|_2^2$ in the binary-aware objective.

2. Apply LLL basis reduction (Lenstra et al., 1982) to basis B_e .

- (a) Fix a parameter $\delta \in (1/4, 1)$, e.g. $\delta = 3/4$.
- (b) Initialize the basis vectors b_1, \dots, b_n as the columns of B_e and compute their Gram–Schmidt orthogonalization:

$$b_i^*, \mu_{i,j}, \quad 1 \leq j < i \leq n,$$

where

$$b_i^* = b_i - \sum_{j < i} \mu_{i,j} b_j^*, \quad \mu_{i,j} = \frac{\langle b_i, b_j^* \rangle}{\langle b_j^*, b_j^* \rangle}.$$

- (c) Set $k \leftarrow 2$.
- (d) While $k \leq n$, perform:
 - i. *Size reduction:* for $j = k - 1, k - 2, \dots, 1$, set

$$m := \text{round}(\mu_{k,j}), \quad b_k \leftarrow b_k - m b_j,$$

and update the Gram–Schmidt data $(b_k^*, \mu_{k,\cdot})$.

- ii. *Lovász condition check:* if

$$\delta \|b_{k-1}^*\|_2^2 \leq \|b_k^*\|_2^2 + \mu_{k,k-1}^2 \|b_{k-1}^*\|_2^2,$$

then set $k \leftarrow k + 1$ (the basis vectors b_{k-1}, b_k are well-ordered). Otherwise (*swap step*):

- Swap the basis vectors: $(b_{k-1}, b_k) \leftarrow (b_k, b_{k-1})$.
 - Recompute Gram–Schmidt data for indices $k - 1$ and k .
 - Set $k \leftarrow \max\{k - 1, 2\}$.
- (e) When the loop terminates, the vectors b_1, \dots, b_n form an LLL-reduced basis. Collect them into the reduced matrix $\tilde{B} \in \mathbb{R}^{(d+n) \times n}$.
 - (f) Keep track of the unimodular transformation $T \in \mathbb{Z}^{n \times n}$ such that $\tilde{B} = B_e T$, i.e., each reduced basis vector is an integer combination of the original ones.

3. Run Babai’s nearest-plane algorithm (Babai, 1986) on the reduced basis \tilde{B} .

- (a) Compute a QR (or Gram–Schmidt) factorization of the reduced basis:

$$\tilde{B} = QR,$$

where $Q \in \mathbb{R}^{(d+n) \times n}$ has orthonormal columns and $R \in \mathbb{R}^{n \times n}$ is upper triangular.

- (b) Compute the coordinates of the target in the orthonormal basis:

$$y := Q^\top t \in \mathbb{R}^n.$$

- (c) Initialize an integer coefficient vector $z \in \mathbb{Z}^n$ (e.g., $z = 0$).
- (d) For $i = n, n-1, \dots, 1$ (backwards):
- i. Compute the one-step residual

$$r_i := y_i - \sum_{j=i+1}^n R_{ij} z_j.$$

- ii. Set

$$z_i := \text{round}\left(\frac{r_i}{R_{ii}}\right),$$

where $\text{round}(\cdot)$ denotes rounding to the nearest integer.

- (e) Map back to the original basis:

$$x_{\text{int}} := Tz \in \mathbb{Z}^n.$$

By construction, $\tilde{B}z = B_e x_{\text{int}}$, so the corresponding lattice vector is

$$y(x_{\text{int}}) = B_e x_{\text{int}} - t = \begin{pmatrix} Vx_{\text{int}} + g^\dagger \\ Mx_{\text{int}} \end{pmatrix}.$$

4. Truncation.

- (a) For M large enough, the integer vector x_{int} produced by the nearest-plane step satisfies $x_{\text{int}} \in \{0, 1\}^n$. In that case, we directly take

$$\hat{x} := x_{\text{int}} \in \{0, 1\}^n$$

as the binary flip pattern.

- (b) If in practice some entries of x_{int} fall outside $\{0, 1\}$, one may optionally project them back to $\{0, 1\}$, e.g.,

$$\hat{x}_i := \min\{1, \max\{0, x_{\text{int},i}\}\}, \quad i = 1, \dots, n.$$

E. BAL-A: Counterexamples for Surrogate Objective Mismatch

Proposition E.1 (No universal M yields minimum-flip recovery). *Fix any $M > 0$. There exist an instance (V, g^\dagger) for which the exact flip attack is feasible with optimal flip count $K^* = 1$, i.e., $\exists x^* \in \{0, 1\}^n$ with $\|x^*\|_0 = 1$ and $Vx^* = -g^\dagger$. But the minimizer of the surrogate problem $\min_{x \in \{0, 1\}^n} F_M(x)$ is infeasible and hence not the optimal attack pattern. Consequently, there is no universal choice of M that guarantees F_M recovers a feasible minimum-flip attack pattern for all instances.*

Proposition E.2 (M can enforce under-selection for any sparsity level). *Fix any integer $K_0 \geq 2$ and any residual scale $r > 0$. There exists an instance (V, g^\dagger) with optimal flip count $K^* = K_0$, i.e., $\exists x^* \in \{0, 1\}^n$ with $\|x^*\|_0 = K_0$ and $Vx^* = -g^\dagger$, such that for any M satisfying $M^2 > r^2$ every minimizer \hat{x} of $\min_{x \in \{0, 1\}^n} F_M(x)$ satisfies $\|\hat{x}\|_0 \leq K_0 - 1$. In particular, minimizing F_M does not recover the minimum-flip solution x^* .*

Proposition E.1 shows that for any fixed M there exist instances where the F_M minimizer is infeasible even though a feasible exact solution exists. This rules out a universal M that guarantees attack success via minimizing F_M . Proposition E.2 is conceptually different: it exhibits instances with any prescribed optimum sparsity $K^* = K_0$ for which the F_M strictly prefers an attack pattern with fewer flips. Together, these results clarify that F_M mixes two goals: (i) promoting binary structure via regularization, (ii) recovering the minimum-flip attack pattern via residual minimization. These goals can conflict, so sufficient conditions tied to each need not admit a common choice of M on a given instance.

F. BAL-A: Worst-Case Performance of BAL-A

We cite the following corollary and definition on the worst-case performance of Babai's algorithm on LLL-reduced bases (Babai, 1986; Stephens-Davidowitz, 2016):

Corollary F.1. *For any $\delta \in (1/4, 1]$, Babai's algorithm with a δ -LLL basis solves γ -CVP for $\gamma \leq \sqrt{n}(\delta - 1/4)^{-n/2}$. In particular, there is an efficient algorithm that solves γ -CVP for $\gamma = 2^{O(n)}$.*

Definition F.2 (γ -CVP). For any approximation factor $\gamma = \gamma(n) \geq 1$, the γ -Closest Vector Problem (γ -CVP) is defined as follows. The input is a basis for a lattice $\mathcal{L} \subseteq \mathbb{R}^n$ and a target vector $t \in \mathbb{R}^n$. The goal is to output a lattice vector $x \in \mathcal{L}$ with $\|x - t\| \leq \gamma \cdot \text{dist}(t, \mathcal{L})$.

G. BMP-A: Full Binary Matching Pursuit Attack Algorithm

We summarize the Binary Matching Pursuit Attack (BMP-A) algorithm in Algorithm 2.

Algorithm 2 Binary Matching Pursuit Attack (BMP-A)

(Modified from (Wen & Li, 2021))

input $V = [v_1, \dots, v_n] \in \mathbb{R}^{d \times n}$, target $y = -g^\dagger \in \mathbb{R}^d$, budget K , tolerance ε
output $x \in \{0, 1\}^n$, residual r

- 2: $r \leftarrow y$, $x \leftarrow 0$, $\Gamma \leftarrow \emptyset$
- 3: **for** $t = 1, 2, \dots, K$ **do**
- 4: $i_t \in \arg \max_{i \in [n] \setminus \Gamma} \frac{|\langle v_i, r \rangle|}{\|v_i\|_2}$
- 5: $\Gamma \leftarrow \Gamma \cup \{i_t\}$, $x_{i_t} \leftarrow 1$
- 6: $r \leftarrow r - v_{i_t}$
- 7: **if** $\|r\|_2 \leq \varepsilon$ **then**
- 8: **break**
- 9: **end if**
- 10: **end for**

H. Experiments and Results: Setup Details

This section collects implementation details omitted from the main text.

H.1. Synthetic Dictionaries

We use synthetic V to test the theory in a controlled way. For BMP-A, the coherence guarantee is stated for a fixed dictionary; therefore we fix a single low-coherence matrix $V \in \mathbb{R}^{200 \times 200}$ and sweep the sparsity level K^* . We build V by repeatedly resampling random Gaussian columns (normalized to unit norm) to reduce the maximum pairwise normalized correlation. The final constructed V has empirical mutual coherence $\mu(V) \approx 0.1971$ and the maximum K^* satisfying the condition (15) is $K_{\text{coh}} = 3$. We then run 200 Monte Carlo trials per K with $K \in \{1, \dots, 60\}$. In each trial we sample a random support S of size K^* as the ground-truth flips x^* , set $-g^\dagger = \sum_{i \in S} v_i$, and run BMP-A for exactly K^* iterations to isolate whether the greedy rule selects the correct support as K^* increases.

For BAL-A, we study the dependence on the lattice penalty M and compare to separation thresholds. Computing the separation threshold requires combinatorial search, so we keep n small. We use a random Gaussian dictionary with unit-norm columns, with $V \in \mathbb{R}^{64 \times 20}$, $K^* = 5$, and 200 Monte Carlo trials. The sufficient binary coefficient bound from (12) gives $M_0 \approx 1.68817$ with $B = 1$ and $R = 0$. The $M_{\text{all sep}}$ that satisfies all separation conditions in (13) is computed exactly as $M_{\text{all sep}} \approx 0.68287$. For each trial we sweep M over 25 log-spaced values in $[0.05, 3.0]$; we apply LLL reduction $\delta = 0.75$ before Babai to improve numerical stability. With $n = 20$, we can enumerate all k -flip candidates for $k < K^*$ and compute the separation threshold exactly, which is why we use this small- n synthetic setting.

H.2. Stanford Human Preferences Dataset

We also evaluate on a real preference dataset, Stanford Human Preferences (SHF) (Ethayarajh et al., 2022), by constructing V from a log-linear DPO pipeline. We load 20,000 training pairs, of which each (history, response) pair is embedded with a frozen DistilBERT encoder (distilbert-base-uncased), using maximum sequence length 256 and the [CLS] embedding. For each preference pair we form the feature difference $\psi_i = \phi(\text{preferred}) - \phi(\text{non-preferred})$. We train a log-linear DPO policy for 3 epochs with learning rate 10^{-3} , batch size 256, and $\beta = 1$. After training, we build the attack matrix V such that each column v_i is the per-example gradient change caused by flipping the i -th preference label.

BAL-A is expensive in the order of n , so on SHF we randomly pick the subset of $n = 50$ for training pairs attack $K^* = 7$ among the subset, and run a penalty sweep over M over 5 trials. The sufficient binary coefficient bound from (12) gives $M_0 \approx 6.71994$ with $B \approx 3.47103$ and $R = 0$. The $M_{\text{all sep}}$ that satisfies all separation conditions in (13) is computed exactly as $M_{\text{all sep}} \approx 1.32166$. We use 25 log-spaced M values in $[0.05, 10.0]$. BAL-A with LLL pre-reduction ($\delta = 0.75$) to attack. Once we obtain the attack output \hat{x} , we evaluate support recovery against x^* .

For BMP-A, we compare two subsets of the *same size* to isolate the effect of coherence: (i) a random subset of training pairs, and (ii) a low-coherence subset selected greedily by adding a column only if its maximum normalized inner product with the already-selected set is below a relaxed threshold. We use $K^* = 10$ and a relaxed threshold larger than that in (15) so that the low-coherence subset is large enough to run many trials. Note that this threshold is not required to satisfy our sufficient condition; it is used only to reduce coherence in practice. On each subset we run 200 Monte Carlo trials: we sample K^* true flips uniformly within the subset, set $t = Vx^*$, run BMP-A with a budget up to $K = K^* + 5 = 15$, and use stopping tolerance $\varepsilon = 10^{-3}$. We report support recovery and residual curves as a function of the budget, and we also report the empirical mutual coherence of each subset to quantify how the subset construction changes V .

We evaluate the ℓ_2 distance of the policy parameter $\hat{\theta}$ learned by DPO on the BAL-A or BMP-A attacked subset of SHP $\tilde{\mathcal{D}}(\hat{x})$ to the parameter θ^\dagger learned on the ground-truth attacked subset of SHP $\tilde{\mathcal{D}}(x^*)$. We also evaluate the ℓ_1 distance of corresponding learned policies $\pi_{\hat{\theta}}$ and π_{θ^\dagger} , to quantify the success of the attack.

I. Experiments and Results: Additional Results on SHP

This section reports the SHP experiments referenced in the main text.

I.1. BAL-A Performance on SHP

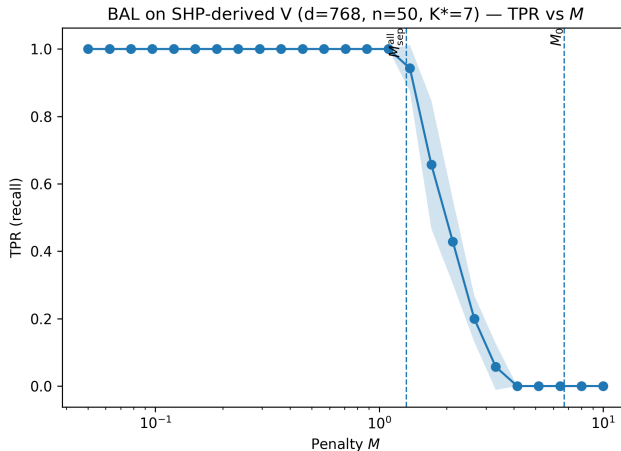


Figure 3. True positive rate of BAL-A on V from SHP as a function of M .

Figure 3 reports TPR of BAL-A on an SHP-derived dictionary ($d = 768$, $n = 50$, $K^* = 7$) as the penalty M varies. Recovery is near-perfect for small M , and then degrades rapidly when M exceeds the separation threshold $M_{\text{sep,all}}$, consistent with the theory. The explicit sufficient bound $M_0 \approx 6.72$ is conservative in this setting.

Figure 4 compares the learned model from the BAL-A attacked subset of SHP $\tilde{\mathcal{D}}(\hat{x})$ to the model learned from the ground-truth attacked subset of SHP $\tilde{\mathcal{D}}(x^*)$, using $\|\hat{\theta} - \theta^\dagger\|_2$ in parameter space and $\|\pi_{\hat{\theta}} - \pi_{\theta^\dagger}\|_1$ in policy space. Across the full sweep of M , both distances change only mildly, even though support recovery in Fig. 3 collapses for large M . This weak dependence is expected in our SHP setting because the learned log-linear DPO model is trained on a limited subset ($n = 50$), so different flip sets can still yield similar fitted parameters/policies. We report these curves to check downstream policy impact, while using TPR as the primary indicator of attack success.

I.2. BMP-A Performance on SHP

Figure 5 shows that the subset construction meaningfully changes the geometry of the SHP-derived dictionary. The random subset has a much heavier right tail of pairwise normalized correlations and a larger mutual coherence (here $\mu \approx 0.807$), while the low-coherence subset shifts the distribution left (here $\mu \approx 0.263$).

Figure 6 compares BMP-A on two SHP-derived dictionaries with the same size ($n = 401$) but different coherence: a random subset ($\mu = 0.807$, $K_{\text{coh}} = 1$) and a low-coherence subset ($\mu = 0.263$, $K_{\text{coh}} = 2$). We sample $K^* = 10$ true flips and set

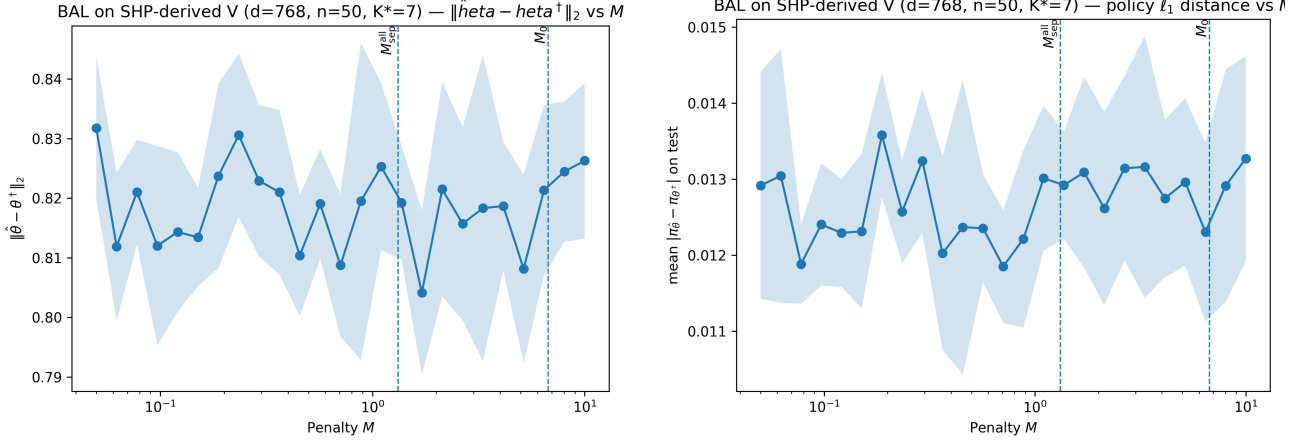


Figure 4. ℓ_2 distance between learned parameters and ℓ_1 distance between learned policies, comparing training on the BAL-A attacked subset $\tilde{\mathcal{D}}(\hat{x})$ versus training on the ground-truth attacked subset $\tilde{\mathcal{D}}(x^*)$, as a function of M .

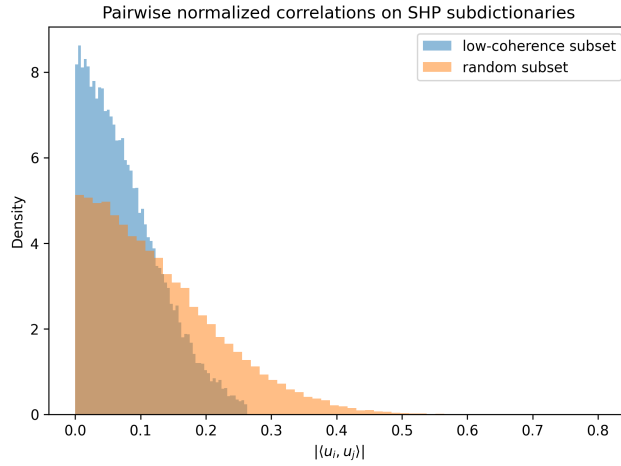


Figure 5. Histogram of pairwise normalized correlations for two subsets of SHP: a random subset and a low-coherence subset.

$y = Vx^*$, then run BMP-A with tolerance $\varepsilon = 10^{-3}$ up to budget $t_{\max} = 15$ with 200 trials. The low-coherence subset yields consistently higher TPR as the budget increases and drives the residual down faster, often reaching a near-zero residual around K^* . In contrast, on the random subset BMP-A makes more incorrect selections as the budget grows, which limits support recovery and can increase the residual after additional wrong updates. Overall, reducing coherence and increasing budget improves the greedy dynamics in practice.

Figure 7 evaluates $\|\hat{\theta} - \theta^\dagger\|_2$ and $\|\pi_{\hat{\theta}} - \pi_{\theta^\dagger}\|_1$ for the BMP-A. Over the sweep on budget K , both quantities change only modestly, even when the recovered support is imperfect. This is reasonable because the DPO model is trained on a larger but still limited subset ($n = 401$), so different flip sets can lead to similar fitted parameters and policies. We include these curves as a sanity check on downstream impact, while using TPR and residual reduction as the primary indicator of attack success.

J. Proofs of Theorems

J.1. Proof of Theorem 3.1

Proof. For the log-linear policy class, we have

$$\log \pi_\theta(a | s) = \psi(s, a)^\top \theta - \log \sum_b \exp(\psi(s, b)^\top \theta),$$

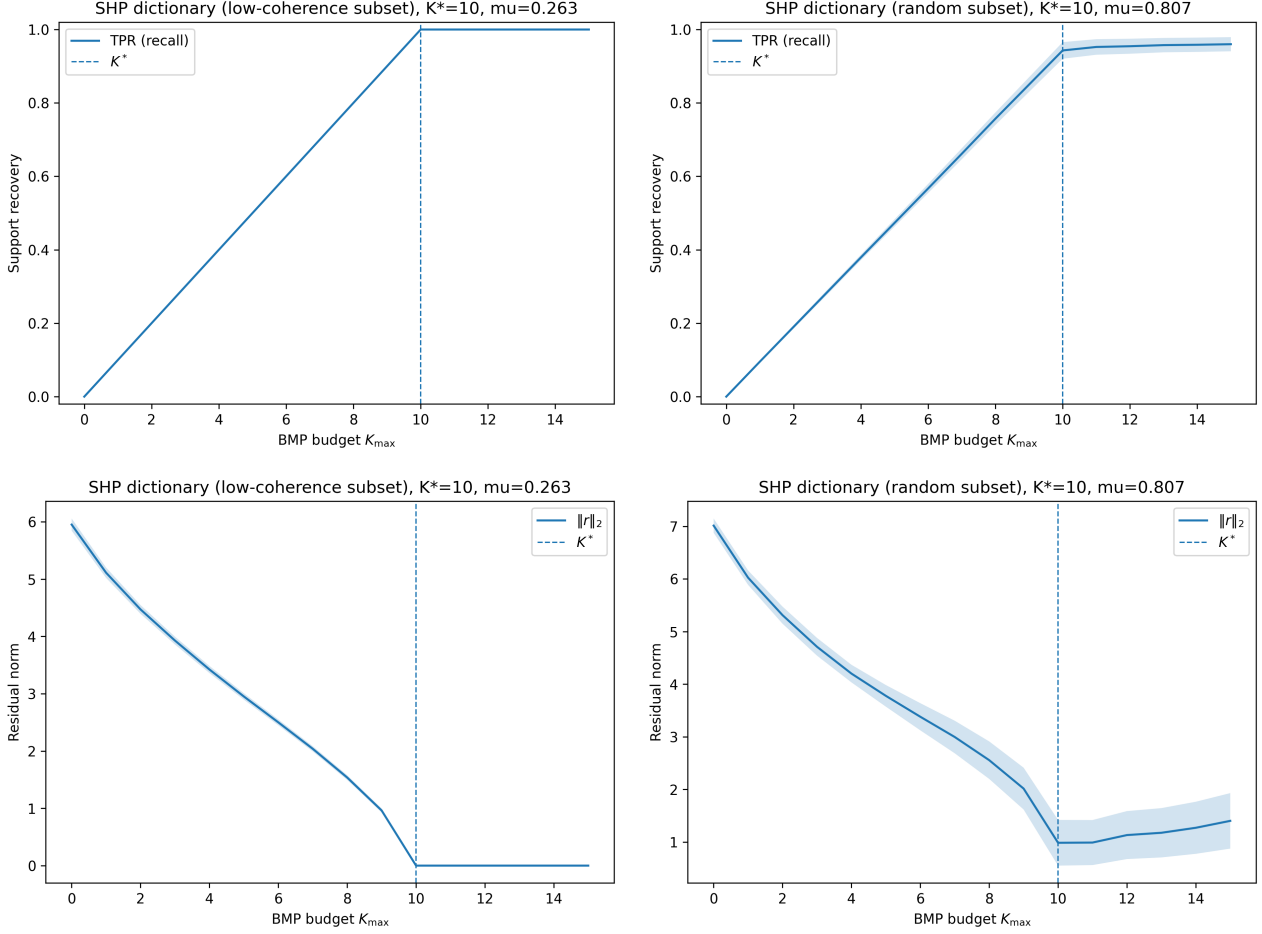


Figure 6. True positive rate and residual of BMP-A on V from different subset of SHP as a function of budget K .

and similarly for $\mu = \pi_{\theta_\mu}$. Therefore,

$$\log \frac{\pi_\theta(a_i | s_i)}{\mu(a_i | s_i)} - \log \frac{\pi_\theta(a'_i | s_i)}{\mu(a'_i | s_i)} = \psi(s_i, a_i)^\top \theta - \psi(s_i, a_i)^\top \theta_\mu - \psi(s_i, a'_i)^\top \theta + \psi(s_i, a'_i)^\top \theta_\mu = \Delta\psi_i^\top (\theta - \theta_\mu),$$

where $\Delta\psi_i := \psi(s_i, a_i) - \psi(s_i, a'_i) \in \mathbb{R}^d$.

Plugging into (1) gives per-sample loss

$$\ell_i(\theta) = -\log \sigma(o_i \beta \Delta\psi_i^\top (\theta - \theta_\mu)) = \log(1 + \exp(-o_i \beta \Delta\psi_i^\top (\theta - \theta_\mu))),$$

since $-\log \sigma(t) = -\log\left(\frac{1}{1+e^{-t}}\right) = \log(1 + e^{-t})$. Differentiating yields the per-sample gradient

$$g_i(\theta) = \nabla \ell_i(\theta) = -o_i \beta \sigma(-o_i \beta \Delta\psi_i^\top (\theta - \theta_\mu)) \Delta\psi_i.$$

Now flip o_i to $\tilde{o}_i = -o_i$. The new per-sample gradient is

$$\tilde{g}_i(\theta) = -\tilde{o}_i \beta \sigma(-\tilde{o}_i \beta \Delta\psi_i^\top (\theta - \theta_\mu)) \Delta\psi_i = o_i \beta \sigma(o_i \beta \Delta\psi_i^\top (\theta - \theta_\mu)) \Delta\psi_i.$$

Hence, the gradient shift is

$$\Delta g_i(\theta) = \tilde{g}_i(\theta) - g_i(\theta) = o_i \beta \sigma(o_i \beta \Delta\psi_i^\top (\theta - \theta_\mu)) \Delta\psi_i + o_i \beta \sigma(-o_i \beta \Delta\psi_i^\top (\theta - \theta_\mu)) \Delta\psi_i.$$

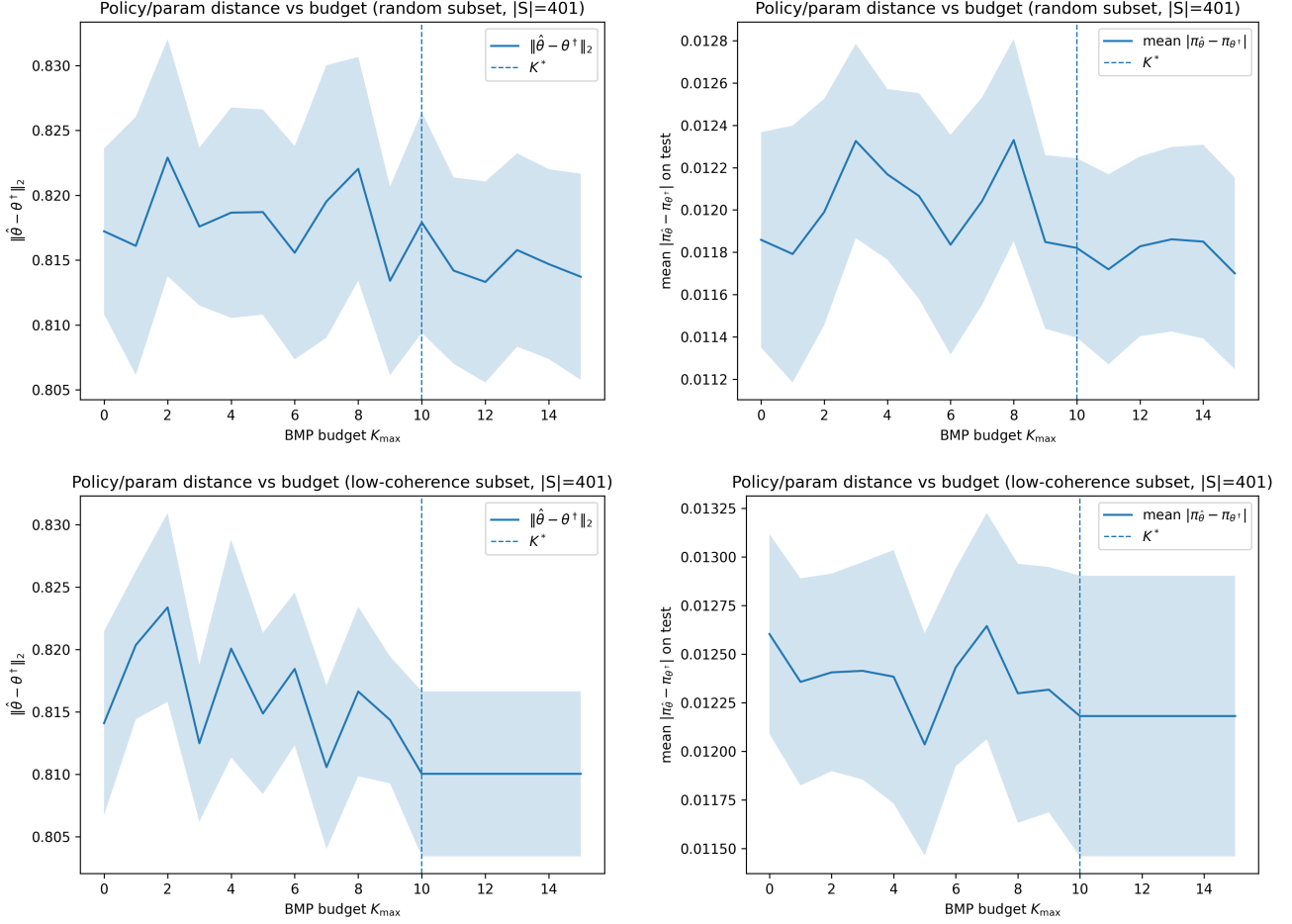


Figure 7. ℓ_2 distance between learned parameters and ℓ_1 distance between learned policies, comparing training on the BMP-A attacked $\tilde{\mathcal{D}}(\hat{x})$ versus training on the ground-truth attacked $\tilde{\mathcal{D}}(x^*)$, as a function of budget K .

Using the sigmoid identity $\sigma(x) = 1 - \sigma(-x)$, we have

$$\Delta g_i(\theta) = o_i \beta \Delta \psi_i =: \Delta g_i.$$

Here we see that the gradient shift caused by flipping the label of one sample is a constant vector, independent of the parameter θ . This proves Theorem 3.1. \square

J.2. Proof of Lemma 3.2

Proof. Let $f(\theta) := L_{\text{DPO}}(\theta; \tilde{\mathcal{D}})$ and $\theta^* := \hat{\theta} = \arg \min_{\theta} f(\theta)$. Since f is μ -strongly convex and differentiable, see Lemma E.14 (Nika et al., 2025), its gradient is μ -strongly monotone: for all θ ,

$$\langle \nabla f(\theta) - \nabla f(\theta^*), \theta - \theta^* \rangle \geq \mu \|\theta - \theta^*\|_2^2.$$

Because θ^* minimizes f , we have $\nabla f(\theta^*) = 0$. Thus,

$$\mu \|\theta - \theta^*\|_2^2 \leq \langle \nabla f(\theta), \theta - \theta^* \rangle \leq \|\nabla f(\theta)\|_2 \|\theta - \theta^*\|_2,$$

where the last inequality is Cauchy–Schwarz.

If $\theta \neq \theta^*$, dividing both sides by $\mu \|\theta - \theta^*\|_2$ yields $\|\theta - \theta^*\|_2 \leq \|\nabla f(\theta)\|_2 / \mu$, and the inequality is trivial when $\theta = \theta^*$.

Taking $\theta = \theta^\dagger$ and using (4) together with (5) gives (6). Finally, Lemma E.5 of (Nika et al., 2025) shows that for log-linear

policies, if $\|\hat{\theta}(x) - \theta^\dagger\|_2 \leq \epsilon/(2\sqrt{d})$, then $\|\pi_{\hat{\theta}(x)} - \pi_{\theta^\dagger}\|_1 \leq \epsilon$. Combining this with (6) yields the stated sufficient condition $\epsilon \leq \mu \epsilon/(2\sqrt{d})$. \square

J.3. Proof of Theorem 3.4

Proof. Recall that we assume that the feature embedding is uniformly bounded, e.g.,

$$\|\psi(s, a)\|_2 \leq 1.$$

Under this assumption, each feature difference satisfies

$$\|\Delta\psi_i\|_2 = \|\psi(s_i, a_i) - \psi(s_i, a'_i)\|_2 \leq 2,$$

and hence each individual flip contribution is bounded as

$$\|o_i\beta\Delta\psi_i\|_2 = \beta\|\Delta\psi_i\|_2 \leq 2\beta.$$

Exact attack. In the exact attack setting, the constraint reads $g^\dagger = \sum_{i \in \mathcal{F}} o_i\beta\Delta\psi_i$. Taking norms and applying the triangle inequality, we obtain

$$\|g^\dagger\|_2 = \left\| \sum_{i \in \mathcal{F}} o_i\beta\Delta\psi_i \right\|_2 \leq \sum_{i \in \mathcal{F}} \|o_i\beta\Delta\psi_i\|_2 \leq \sum_{i \in \mathcal{F}} 2\beta = 2\beta|\mathcal{F}|. \quad (19)$$

Consequently,

$$|\mathcal{F}| \geq \frac{\|g^\dagger\|_2}{2\beta}. \quad (20)$$

Approximate attack. In the approximate case, we allow that $\|g^\dagger + \sum_{i \in \mathcal{F}} o_i\beta\Delta\psi_i\|_2 \leq \epsilon$. Applying the reverse triangle inequality to the summation term, we have

$$\left\| \sum_{i \in \mathcal{F}} o_i\beta\Delta\psi_i \right\|_2 \geq \|g^\dagger\|_2 - \epsilon.$$

On the other hand, as in (19), we also have

$$\left\| \sum_{i \in \mathcal{F}} o_i\beta\Delta\psi_i \right\|_2 \leq 2\beta|\mathcal{F}|.$$

Combining these inequalities yields

$$\|g^\dagger\|_2 - \epsilon \leq 2\beta|\mathcal{F}|,$$

so that

$$|\mathcal{F}| \geq \frac{\|g^\dagger\|_2 - \epsilon}{2\beta}. \quad (21)$$

\square

J.4. Proof of Lemma 4.1

The proof is a local-improvement argument: if some coefficient were ≥ 2 , reducing it by one decreases the penalty by at least $3M^2$, while the residual term can increase by at most $O(B\|r\|) + O(B^2)$; choosing M large ensures the penalty decrease dominates, contradicting optimality.

Proof. First, by feasibility of x^* and optimality of x^{opt} ,

$$\|y(x^{\text{opt}})\|_2^2 \leq \|y(x^*)\|_2^2 = \|Vx^* + g^\dagger\|_2^2 + M^2\|x^*\|_2^2 \leq R^2 + M^2K^*. \quad (22)$$

Let

$$r := Vx^{\text{opt}} + g^\dagger \in \mathbb{R}^d.$$

Then from (22) and $\|y(x^{\text{opt}})\|_2^2 = \|r\|_2^2 + M^2\|x^{\text{opt}}\|_2^2 \geq \|r\|_2^2$, we get

$$\|r\|_2 \leq \sqrt{R^2 + M^2K^*}. \quad (23)$$

We now show that for M large enough, x^{opt} cannot have any coordinate with magnitude at least 2. Suppose for contradiction that there exists an index j with $|x_j^{\text{opt}}| \geq 2$. Let $s := \text{sign}(x_j^{\text{opt}}) \in \{-1, +1\}$ and define the perturbed integer vector

$$\tilde{x} := x^{\text{opt}} - se_j,$$

where e_j is the j -th standard basis vector. Define the corresponding residual

$$\tilde{r} := V\tilde{x} + g^\dagger = r - sv_j.$$

Step 1 (bound the change in the top term). Compute

$$\|\tilde{r}\|_2^2 = \|r - sv_j\|_2^2 = \|r\|_2^2 - 2s\langle r, v_j \rangle + \|v_j\|_2^2,$$

hence

$$\|r\|_2^2 - \|\tilde{r}\|_2^2 = 2s\langle r, v_j \rangle - \|v_j\|_2^2.$$

Taking absolute values and using the triangle inequality (and $|s| = 1$),

$$\left| \|r\|_2^2 - \|\tilde{r}\|_2^2 \right| = |2s\langle r, v_j \rangle - \|v_j\|_2^2| \leq 2|\langle r, v_j \rangle| + \|v_j\|_2^2.$$

By Cauchy–Schwarz,

$$|\langle r, v_j \rangle| \leq \|r\|_2 \|v_j\|_2,$$

so

$$\left| \|r\|_2^2 - \|\tilde{r}\|_2^2 \right| \leq 2\|r\|_2 \|v_j\|_2 + \|v_j\|_2^2.$$

Finally, using $\|v_j\|_2 \leq B$ yields

$$\left| \|r\|_2^2 - \|\tilde{r}\|_2^2 \right| \leq 2B\|r\|_2 + B^2. \quad (24)$$

Using (23), we further obtain

$$\left| \|r\|_2^2 - \|\tilde{r}\|_2^2 \right| \leq 2B\sqrt{R^2 + M^2K^*} + B^2. \quad (25)$$

Step 2 (exact change in the bottom penalty). Since only the j -th coordinate changes,

$$\|x^{\text{opt}}\|_2^2 - \|\tilde{x}\|_2^2 = (x_j^{\text{opt}})^2 - (x_j^{\text{opt}} - s)^2 = (x_j^{\text{opt}})^2 - ((x_j^{\text{opt}})^2 - 2sx_j^{\text{opt}} + 1) = 2sx_j^{\text{opt}} - 1 = 2|x_j^{\text{opt}}| - 1.$$

Because $|x_j^{\text{opt}}| \geq 2$, we have $2|x_j^{\text{opt}}| - 1 \geq 3$, hence

$$M^2(\|x^{\text{opt}}\|_2^2 - \|\tilde{x}\|_2^2) \geq 3M^2. \quad (26)$$

Step 3 (combine and enforce positivity). By definition,

$$\|y(x^{\text{opt}})\|_2^2 - \|y(\tilde{x})\|_2^2 = (\|r\|_2^2 - \|\tilde{r}\|_2^2) + M^2(\|x^{\text{opt}}\|_2^2 - \|\tilde{x}\|_2^2).$$

Using (25) and (26),

$$\|y(x^{\text{opt}})\|_2^2 - \|y(\tilde{x})\|_2^2 \geq 3M^2 - \left(2B\sqrt{R^2 + M^2K^*} + B^2\right). \quad (27)$$

If the right-hand side of (27) is strictly positive, then $\|y(\tilde{x})\|_2^2 < \|y(x^{\text{opt}})\|_2^2$, contradicting optimality of x^{opt} .

A sufficient (explicit) way to ensure positivity is to upper bound $\sqrt{R^2 + M^2K^*} \leq R + M\sqrt{K^*}$, which yields the condition

$$3M^2 > 2B(R + M\sqrt{K^*}) + B^2.$$

Equivalently,

$$3M^2 - 2B\sqrt{K^*}M - (2BR + B^2) > 0,$$

which holds whenever M exceeds the positive root of this quadratic, giving (12). Thus, for all such M , no coordinate of x^{opt} can satisfy $|x_j^{\text{opt}}| \geq 2$. Therefore $x^{\text{opt}} \in \{-1, 0, 1\}^n$. \square

J.5. Proof of Theorem 4.2

Proof. By Lemma 4.1, every minimizer over \mathbb{Z}^n satisfies $|x_i| \leq 1$ for all i when $M \geq M_0$. Under the additional restriction $x_i \geq 0$, this implies $x_i \in \{0, 1\}$ for all i , hence $x^{\text{opt}} \in \{0, 1\}^n$. The objective bound follows from feasibility of x^* and optimality of x^{opt} : $\|y(x^{\text{opt}})\|_2^2 \leq \|y(x^*)\|_2^2 \leq R^2 + M^2 K^*$. \square

J.6. Proof of Theorem 4.3

Proof. Since x^* is feasible, $F_M(x^*) = M^2 K^*$. Consider any $x \in \{0, 1\}^n$. If $\mathbf{1}^\top x \geq K^*$, then $F_M(x) \geq M^2 \mathbf{1}^\top x \geq M^2 K^* = F_M(x^*)$.

If $\mathbf{1}^\top x = k < K^*$, then by definition of ρ_k ,

$$F_M(x) \geq \rho_k^2 + M^2 k.$$

Under (13), $\rho_k^2 + M^2 k > M^2(K^* - k) + M^2 k = M^2 K^* = F_M(x^*)$. Hence no k -flip vector with $k < K^*$ can minimize F_M , and no vector with $k \geq K^*$ can do better than x^* either. Therefore any minimizer must have $\mathbf{1}^\top x = K^*$ and satisfy $Vx + g^\dagger = 0$, i.e., it is an optimal exact attack pattern. \square

J.7. Proof of Proposition E.1

Proof. Fix any $M > 0$. Choose any dimension $d \geq 1$ and any $n \geq 1$. Let $g^\dagger \in \mathbb{R}^d$ be any nonzero vector with

$$\|g^\dagger\|_2 = \frac{M}{2} < M.$$

Construct $V \in \mathbb{R}^{d \times n}$ whose first column is

$$v_1 := -g^\dagger,$$

and whose remaining columns are arbitrary.

Then the exact flip attack is feasible with the binary vector $x^* = e_1 \in \{0, 1\}^n$:

$$Vx^* = v_1 = -g^\dagger,$$

so the optimal flip count is $K^* = \|x^*\|_0 = 1$.

Now consider the surrogate objective $F_M(x) = \|Vx + g^\dagger\|_2^2 + M^2 \mathbf{1}^\top x$ over $x \in \{0, 1\}^n$. For the zero vector,

$$F_M(0) = \|g^\dagger\|_2^2 = \frac{M^2}{4}.$$

For any $x \neq 0$ with $x \in \{0, 1\}^n$, we have $\mathbf{1}^\top x \geq 1$, hence

$$F_M(x) = \|Vx + g^\dagger\|_2^2 + M^2 \mathbf{1}^\top x \geq 0 + M^2 > \frac{M^2}{4} = F_M(0).$$

Therefore, the unique minimizer of $\min_{x \in \{0, 1\}^n} F_M(x)$ is $\hat{x} = 0$.

Finally, since $g^\dagger \neq 0$, $\hat{x} = 0$ is infeasible for the exact attack constraint $Vx + g^\dagger = 0$ (it yields residual $\|g^\dagger\|_2 > 0$), whereas a feasible exact solution exists with one flip. This shows that for the fixed M we constructed an instance where minimizing F_M fails to recover a feasible minimum-flip exact attack. Since $M > 0$ was arbitrary, no universal choice of M can guarantee minimum-flip recovery for all instances. \square

J.8. Proof of Proposition E.2

Proof. Fix $K_0 \geq 2$ and $r > 0$. Choose any $d \geq K_0$ and any $n \geq K_0$. Construct a dictionary whose first K_0 columns are orthogonal vectors with equal norm r :

$$v_1, \dots, v_{K_0} \in \mathbb{R}^d, \quad \langle v_i, v_j \rangle = 0 \ (i \neq j), \quad \|v_i\|_2 = r.$$

(The remaining columns, if any, are arbitrary.) Define

$$x^* = \sum_{i=1}^{K_0} e_i \in \{0, 1\}^n, \quad K^* = \|x^*\|_0 = K_0,$$

and set the noiseless target

$$-g^\dagger = Vx^* = \sum_{i=1}^{K_0} v_i.$$

Then x^* is feasible and achieves zero residual, hence using $\|x^*\|_2^2 = \|x^*\|_0 = K_0$,

$$F_M(x^*) = 0 + M^2 K_0.$$

Now consider the $(K_0 - 1)$ -flip candidate $x' = \sum_{i=1}^{K_0-1} e_i$. Its residual is

$$Vx' - (-g^\dagger) = \sum_{i=1}^{K_0-1} v_i - \sum_{i=1}^{K_0} v_i = -v_{K_0},$$

so $\|Vx' - (-g^\dagger)\|_2^2 = \|v_{K_0}\|_2^2 = r^2$, and $\|x'\|_2^2 = K_0 - 1$. Therefore,

$$F_M(x') = r^2 + M^2(K_0 - 1).$$

Comparing $F_M(x')$ and $F_M(x^*)$,

$$F_M(x') < F_M(x^*) \iff r^2 + M^2(K_0 - 1) < M^2 K_0 \iff M^2 > r^2.$$

Hence for any M satisfying $M^2 > r^2$, the K_0 -flip solution x^* cannot minimize F_M , and every minimizer \hat{x} must satisfy $\|\hat{x}\|_0 \leq K_0 - 1$. \square

J.9. Proof of Theorem 5.3

Proof. We follow the proof of Theorem 1 in Appendix B of (Wen & Li, 2021) and only record the substitutions needed to match our non-normalized BMP-A.

Notation substitutions. Replace the unit-norm dictionary columns A_i in (Wen & Li, 2021) by the normalized directions $u_i := v_i / \|v_i\|_2$, and denote $U := [u_1, \dots, u_n]$. Replace the measurement model $y = Ax^* + v$ by our target y together with the residual noise $e := y - Vx^*$ (so $\|e\|_2 \leq \varepsilon$ by Assumption 5.1). Replace their sparsity level K by K^* , their tolerance δ by ε , and their coherence $\mu(A) = \max_{i \neq j} |A_i^\top A_j|$ by $\mu(V) := \max_{i \neq j} |\langle u_i, u_j \rangle|$. Finally, introduce the column-norm range $b := \min_i \|v_i\|_2$ and $B := \max_i \|v_i\|_2$.

Changes to Appendix B inequalities. The greedy selection rule of BMP-A is

$$i_k \in \arg \max_{i \notin \Gamma_{k-1}} \frac{|\langle v_i, r^{k-1} \rangle|}{\|v_i\|_2} = \arg \max_{i \notin \Gamma_{k-1}} |\langle u_i, r^{k-1} \rangle|,$$

so (B1) in Appendix B of (Wen & Li, 2021) becomes

$$\|U_{\Omega \setminus \Gamma_{k-1}}^\top r^{k-1}\|_\infty > \|U_{\Omega^c}^\top r^{k-1}\|_\infty.$$

The residual decomposition (B2) is replaced by the exact identity implied by our update $r \leftarrow r - v_i$:

$$r^{k-1} = y - \sum_{i \in \Gamma_{k-1}} v_i = \sum_{i \in \Omega \setminus \Gamma_{k-1}} v_i + e = \sum_{i \in \Omega \setminus \Gamma_{k-1}} \|v_i\|_2 u_i + e.$$

With these substitutions, the derivation of (B3) is unchanged, except that every occurrence of $A^\top(\cdot)$ is replaced by $U^\top(\cdot)$ and $A_{\Omega \setminus \Gamma} x_{\Omega \setminus \Gamma}$ is replaced by $V_{\Omega \setminus \Gamma} \mathbf{1}$, since x^* is binary on the remaining support.

The two key bounds (B4) and (B5) in Appendix B of (Wen & Li, 2021) now read

$$\|U_{\Omega \setminus \Gamma}^\top V_{\Omega \setminus \Gamma} \mathbf{1}\|_\infty \geq b - (|\Omega \setminus \Gamma| - 1)\mu(V)B \quad \text{and} \quad \|U_{\Omega^c}^\top V_{\Omega \setminus \Gamma} \mathbf{1}\|_\infty \leq |\Omega \setminus \Gamma|\mu(V)B,$$

since $\langle u_i, v_i \rangle = \|v_i\|_2 \geq b$ and $|\langle u_i, v_j \rangle| = \|v_j\|_2 |\langle u_i, u_j \rangle| \leq B\mu(V)$ for $i \neq j$. The noise bound (B6) is unchanged because $\|u_i\|_2 = 1$:

$$\|U_{\Omega \setminus \Gamma}^\top e\|_\infty + \|U_{\Omega^c}^\top e\|_\infty \leq 2\|e\|_2 \leq 2\varepsilon.$$

Combining these bounds yields the same correlation gap as in Appendix B of (Wen & Li, 2021) provided that

$$b - (2K^* - 1)\mu(V)B > 2\varepsilon > 0,$$

which is exactly (15)–(16). Therefore, BMP-A selects an index in $\Omega = \text{supp}(x^*)$ at each iteration, and after K^* iterations it recovers $\text{supp}(x^*)$.

Finally, once $\text{supp}(\hat{x}) = \text{supp}(x^*)$, we have $r^{K^*} = y - V\hat{x} = y - Vx^* = e$, so $\|r^{K^*}\|_2 \leq \varepsilon$ and the stopping rule triggers no later than iteration K^* . \square

J.10. Proof of Theorem 5.4

Proof. We prove impossibility by upper bounding the largest gradient shift $\|Vx\|_2$ achievable with at most K flips, and comparing it to the amount of shift needed to reach tolerance ε .

Suppose there exists a binary vector $x \in \{0, 1\}^n$ with $\|x\|_0 \leq K$ such that $\|Vx + g^\dagger\|_2 \leq \varepsilon$. Let $r := Vx + g^\dagger$. By the reverse triangle inequality,

$$\|Vx\|_2 \geq \|g^\dagger\|_2 - \|r\|_2 \geq \|g^\dagger\|_2 - \varepsilon. \quad (28)$$

Thus any successful K -flip attack must produce a shift of size at least $\|g^\dagger\|_2 - \varepsilon$.

Spectral norm impossibility (17). Since x is binary with at most K ones, we have $\|x\|_2 = \sqrt{\|x\|_0} \leq \sqrt{K}$. Therefore,

$$\|Vx\|_2 \leq \|V\|_2 \|x\|_2 \leq \|V\|_2 \sqrt{K}.$$

Combining with (28) yields

$$\|g^\dagger\|_2 - \varepsilon \leq \|V\|_2 \sqrt{K},$$

which contradicts (17).

Coherence impossibility (18). Let $S := \text{supp}(x)$ so that $|S| = \|x\|_0 \leq K$ and $Vx = \sum_{i \in S} v_i$. Write $v_i = a_i u_i$ with $a_i = \|v_i\|_2$ and $\|u_i\|_2 = 1$. Expanding the squared norm and using $|\langle u_i, u_j \rangle| \leq \mu(V)$ gives

$$\begin{aligned} \|Vx\|_2^2 &= \left\langle \sum_{i \in S} a_i u_i, \sum_{j \in S} a_j u_j \right\rangle = \sum_{i \in S} a_i^2 + \sum_{\substack{i, j \in S \\ i \neq j}} a_i a_j \langle u_i, u_j \rangle \\ &\leq \sum_{i \in S} a_i^2 + \mu(V) \sum_{\substack{i, j \in S \\ i \neq j}} a_i a_j \leq |S|B^2 + \mu(V) |S|(|S| - 1)B^2 \leq B^2 \left(K + \mu(V) K(K - 1) \right). \end{aligned} \quad (29)$$

Together with (28), this implies

$$\left(\|g^\dagger\|_2 - \varepsilon \right)^2 \leq B^2 \left(K + \mu(V) K(K - 1) \right),$$

which contradicts (18). This completes the proof. \square